Measurement of Henry's law and liquid-phase loss rate constants of peroxypropionic nitric anhydride (PPN) in deionized water and in n-octanol

Kevin D. Easterbrook,[1] Mitchell A. Vona,[1] Kiana Nayebi-Astaneh,[1] Amanda M. Miller,[1] and Hans D. Osthoff[1]

[1] Department of Chemistry, University of Calgary, 2500 University Drive N.W., Calgary, Alberta, Canada T2N 1N4

Correspondence to: Hans D. Osthoff (hosthoff@ucalgary.ca)

for *Atmos. Chem. Phys.*

Abstract

The Henry's law solubility (H_S) and liquid-phase loss rate constants (k_l) of the tropospheric trace gas

15   constituents peroxyacetic nitric anhydride (PAN, $CH_3C(O)O_2NO_2$; commonly known as peroxyacetyl nitrate) and peroxypropionic nitric anhydride (PPN, $C_2H_5C(O)O_2NO_2$; also known as peroxypropionyl nitrate) in deionized (DI) water and of PPN in n-octanol were measured using a flow bubble apparatus at temperatures between 5.0 °C and 25.0 °C. For PAN in DI water, the observed values for $H_{S,aq}$ are consistent with literature, whereas the solubility of PPN in DI water is slightly lower than literature values, ranging

20   from $H_S^{CPcp}(\text{PPN})_{aq} = (1.49\pm0.05)$ M atm^{-1} at 25.0 °C to $H_S^{CPcp}(\text{PPN})_{aq} = (7.01\pm0.25)$ M atm^{-1} at 5.0 °C (stated uncertainties are at the 1σ level). The data are best described by $\ln(H_S^{CPcp}(\text{PAN})_{aq}/[\text{M atm}^{-1}]) = -(17.8\pm0.3) + (5620\pm85)/T$ and $\ln(H_S^{CPcp}(\text{PPN})_{aq}/[\text{M atm}^{-1}]) = -(19.5\pm1.7) + (5955\pm480)/T$ where T is in Kelvin. For n-octanol, the PPN solubility ranges from $H_S^{CPcp}(\text{PPN})_{oct} = (88\pm5)$ M atm^{-1} at 25.0 °C to $H_S^{CPcp}{}_{oct} = (204\pm16)$ M atm^{-1} at 5.0 °C and is best described by

25   $\ln(H_S^{CPcp}(\text{PPN})_{oct}/[\text{M atm}^{-1}]) = -(6.92\pm0.75) + (3390\pm320)/T$. n-Octanol-water partition coefficients (K_{OW}) for PPN were determined for the first time, ranging from 59±4 at 25.0 °C to 29±3 at 5.0 °C. Observed loss rate constants in DI water are consistent with recent literature and larger than the thermal dissociation rates for both PAN and PPN, consistent with a hydrolysis mechanism, whereas k_l values in n-octanol are significantly smaller than gas-phase dissociation rate constants, likely owing to a "cage effect" in the

30   organic liquid. The results imply that uptake of either PAN or PPN on cloud water and organic aerosol is negligible but that uptake of PPN may constitute an overlooked source of peroxy radicals in organic aerosol.

INTRODUCTION

The peroxycarboxylic nitric anhydrides (PANs; also referred to as peroxyacyl nitrates, molecular formula $RC(O)O_2NO_2$, $R \neq H$) are important trace gas constituents of the troposphere (Roberts, 1990, 2007; Gaffney and Marley, 2021). Formed as by-products by the same photochemistry that produces ozone (O_3) and photochemical smog, the relative abundances of PANs allow insights into the dominant hydrocarbons involved in the O_3-production process (Williams et al., 1997; Roberts et al., 2007). Their formation and fate affects the budgets of nitrogen oxides (i.e., $NO_x = NO+NO_2$) and the abundances of radicals such as the hydroxyl radical (OH), the hydroperoxyl radical (HO_2) and organic peroxy radicals (RO_2) and, ultimately, O_3 and aerosol production rates (Roberts, 1990, 2007). The phytotoxic PANs are prone to thermal decomposition in warm climates but are longer-lived in parts of the troposphere where temperatures are lower. For the two most abundant PANs, peroxyacetic and peroxypropanoic nitric anhydride (PAN and PPN, often referred to as peroxyacetyl and peroxypropionyl nitrate, respectively), the ~~Since their~~ rate constants for photolysis and reaction with OH are relatively small ($< 5 \times 10^{-7}$ s^{-1}) in the ~~lower~~ troposphere (Talukdar et al., 1995; Harwood et al., 2003). Further, because the products of PAN (or PPN) photolysis may recombine and regenerate PAN (or PPN), their effective lifetimes are often much larger than suggested by these loss rate constants. For example, Harwood et al. (2003) calculated an effective lifetime of 4 months in the upper troposphere. ~~Hence~~Under these conditions, dissolution in cloud or fog droplets followed by hydrolysis (Roberts et al., 1996; McFadyen and Cape, 1999) or stomatal uptake (Sparks et al., 2003; Teklemariam and Sparks, 2004) ~~then~~ constitute potential loss pathways. Hence, knowledge of their temperature-dependent Henry's law (H) and loss rate constants (k_l) for both aqueous and non-polar liquid phases is of interest.

There are several variants of H constants in use (Sander et al., 2022). From a thermodynamic point of view, the dimensionless Henry's law solubility constant (H_S^{ccc}), defined as the ratio of liquid over gas-phase concentration, is preferred. Atmospheric chemists typically use Henry solubility in units of M atm^{-1} ($H_S^{\text{cp}cp}$; for simplicity, referred to as H in the remainder of this manuscript), which is defined as the ratio of liquid-phase concentration (in M) over the partial pressure (in atm) and is related to H_S^{ccc} by:

$$HRT = H_S^{\text{ccc}} \tag{1}$$

Here, T is the temperature in Kelvin, and R is the universal gas constant (0.08205 L atm mol^{-1} K^{-1}). As summarized in Appendix B of Staudinger and Roberts (2001), the temperature dependence of H is related to the enthalpy and entropy of solvation, ΔH_{sol}^0 and ΔS_{sol}^0, and is often described using a Van't Hoff-type equation, i.e.,

$$\ln\left(H_S^{\text{ccc}}\right) = \frac{\Delta S_{sol}^0}{R} - \frac{\Delta H_{sol}^0}{RT}, \tag{2}$$

or, if H (i.e., H_S^{CPcp}) is used:

$$\ln(H) = A_H - \frac{B_H}{T} + C_H ln(T) \approx A_H - \frac{B_H}{T}. \tag{3}$$

Here, A_H, B_H and C_H are simple curve-fitting parameters. Equation (3) is used to parameterize H constants
70 by the National Aeronautics and Space Administration Jet Propulsion Laboratory (NASA-JPL) evaluation
panel of chemical kinetics data for use in atmospheric studies (Burkholder et al., 2020). Because ΔS_{sol}^0 and
ΔH_{sol}^0 (and hence A_H and B_H) for the PANs are not significantly temperature-dependent in the range of
interest to atmospheric chemists, the third term is usually omitted (i.e., C_H=0) (Burkholder et al., 2020).

For the most abundant of the PANs, ~~peroxyacetic nitric anhydride (~~PAN~~; often referred to as peroxyacetyl~~
75 ~~nitrate)~~, H and k_1 constants in deionized (DI) water have been measured over a range of temperatures
pertinent to the lower troposphere in a handful of studies (Kames and Schurath, 1995; Kames et al., 1991;
Holdren et al., 1984; Frenzel et al., 2000; Lee, 1984). Measurements below room temperature are of
particular interest because fog droplets and clouds (which can act as sinks for PANs) are generally more
prevalent under those conditions (Koracin et al., 2001). For the second most abundant of the PANs,
80 ~~peroxypropionic nitric anhydride (~~PPN~~, often referred to as peroxypropionyl nitrate)~~, in contrast, there has
only been a single study measuring H and k_1 constants in DI water (Kames and Schurath, 1995), though it
is clear from these data that the uptake of PAN and PPN on cloud droplets is negligible. Nevertheless,
significant enhancements in the PPN:PAN ratio has been observed in fog-processed air in New England
(Roberts et al., 1996), rationalized at least in part by reactive uptake of the peroxyacetyl (PA) radical
85 (formed from thermal dissociation of PAN) on fog droplets that is faster than the reformation of PAN via
PA + NO$_2$ (Villalta et al., 1996).

The Henry's law solubility and liquid-phase loss rate constants of PAN in n-octanol have been reported by
Roberts (2005) to gain insight into this molecule's potential uptake on organic aerosol and non-polar
stomatal media. Analogous data for PPN do not exist, though PPN likely exhibits greater partitioning to
90 organic phases than PAN because of its larger aliphatic side chain. Knowledge of the air-octanol and air-
water partitioning constants allows the widely used octanol-water partition coefficient (K_{OW}) to be
calculated:

$$K_{OW} = \frac{H_S^{CCcc}(\text{octanol})}{H_S^{CCcc}(\text{aq})} = \frac{H_S^{CPcp}(\text{octanol})}{H_S^{CPcp}(\text{aq})} \tag{4}$$

This constant provides a direct estimate of hydrophobicity and of partitioning of a molecule from water to
95 organic media such as lipids, waxes, and natural organic matter, including organic aerosol (Mackay and
Parnis, 2020), but has not been previously determined for PPN.

In this work, we report the H and k_l constants for PAN and PPN in DI water to corroborate the data by Kames and Schurath (1995) and for PPN in n-octanol at temperatures between 5.0 °C and 25.0 °C. We calculate K_{OW} values for PPN and estimate rates for its wet deposition and uptake rates on organic aerosol in the atmosphere.

METHODS

Aliquots of PAN (or PPN) in tridecane solution were synthesized from reaction of acidified peroxycarboxylic acid solutions with concentrated nitric acid (Mielke and Osthoff, 2012; Williams et al., 2000) and stored in a freezer until use.

Gas streams containing PAN or PPN in nitrogen (N_2) were generated using diffusion sources as described by Furgeson et al. (2011) and depicted within the dashed box in Figure 1. At the start of each experiment, a solution containing PAN (or PPN) was placed in a 3-neck glass vessel submerged into a dewar containing an ice-water bath. The N_2 gas flow was set to ~40 standard (0 °C, 1 bar) cubic centimeters per minute (sccm) via a 50 μm diameter critical orifice (Lenox Laser) and a regulator back pressure of 25 pounds per square inch (psi, 1.7 bar). The source of the N_2 gas was the "blow-off" from a liquid N_2 dewar (not shown), chosen because of its high purity. The output of the diffusion source was directed to a fume hood via a 2-way perfluoroalkoxy (PFA) Teflon valve (Swagelok) and allowed to stabilize over a period of several hours.

Henry's law solubility and liquid-phase loss rate constants were measured using a jacketed, Pyrex bubble column apparatus (internal volume ~175 mL, diameter ~4.5 cm, height ~35 cm; Figure 1) similar to those described by Kames and Schurath (1995) and Roberts (2005). The gas-phase PAN (or PPN) concentration downstream of the bubble column was monitored by a gas chromatograph with electron capture detector (GC-ECD) which sampled at an inlet flow rate of 75 sccm. The Varian GC-ECD described by Tokarek et al. (2014) was used for most of the experiments (see schedule in Tables S1-S4 in the supporting information (S.I.) section), though some measurements were also carried out using the Hewlett Packard (HP) GC described in (Rider et al., 2015; Zborowska et al., 2021). The Varian GC-ECD was equipped with a 30 m long megabore column (Restek RTX-1701, film thickness 1 μm) and a 0.5 mL stainless steel sample loop (VICI Cheminert). It was operated at an oven temperature of 25 °C, an ECD temperature of ~100 °C, with N_2 carrier gas (from the aforementioned liquid N_2 dewar) at a carrier gas flow rate of ~40 mL min^{-1}, and a make-up gas flow rate of ~8.1 mL min^{-1}. The HP GC-ECD was equipped with a 15 m long megabore column (Restek RTX-200, film thickness 1 μm) and a 2.0 mL stainless steel sample loop (VICI Cheminert). It was also operated at an oven temperature of at 25 °C and at an ECD temperature of 105 °C, but with helium (He) carrier gas at a flow rate of ~19.4 mL min^{-1} and N_2 make-up gas at a flow rate of ~44.0 mL

min^{-1}. The GCs were set to automatically inject every 120 s for experiments with PAN or every 360 s for experiments with PPN. For experiments with PAN, ~~connecting tubing and fittings were constructed from~~ fluorinated ethylene propylene (FEP) ~~Teflon~~ tubing (Saint-Gobain) and PFA Teflon fittings (Entegris) were used, and the GC sampled through a PFA Teflon filter (Pall, 2 μm pore size) housed in a PFA Teflon in-line filter holder (Cole-Parmer RK-06103-13). For experiments with PPN, tubing downstream of the bubble column were replaced with 1/8" (~0.32 cm) outer diameter (o.d.) stainless tubing and fittings (Swagelok), and the GC inlet filter and holder were removed because of memory effects with the ~~Teflon~~ fluoropolymer tubing and fittings.

In a typical experiment, the bubble column apparatus (right-hand side of Figure 1) was filled with a known volume (V_l) of liquid solution, i.e., either DI water (18 MΩ cm^{-1}, Thermo Scientific Barnstead Nanopure Model D11931) or n-octanol (ACS reagent grade, ≥99% purity, used as received). This apparatus was temperature-controlled using an external chiller-circulator (Lauda Proline RP 1290 for experiments with the Varian GC-ECD, or VWR 13271-100 for experiments with the HP GC-ECD). Once the desired temperature was achieved, the gas stream containing PAN (or PPN) was bubbled through the water (or n-octanol) by opening the 2-way valve (top of Figure 1) and closing the 2-way valve connected to the waste line. After ~ 5 min the incoming gas stream was directed towards a waste line (by opening the 2-way valve connected to it). Gas-phase PAN (or PPN) mixing ratios ~~(c_g)~~ ranged from ~10 ppbv to ~300 ppbv at this stage. For experiments with PPN, the tee fitting was briefly (~30 s) back-flushed with N$_2$ delivered via a calibrated mass flow controller (MFC, MKS Instruments, 500 sccm capacity for experiments with the Varian GC-ECD, 5000 sccm capacity for experiments with the HP GC-ECD) until the 2-way valve connecting the source to the bubble column apparatus and N$_2$ flow was closed. For experiments with DI water, the N$_2$ flow was humidified using a bubbler to minimize evaporation of solvent in the main bubble column. The PAN (or PPN) concentration ~~decay~~ (c_g) was then monitored as a function of time (t) by either GC. The experiment was repeated, systematically varying the (volumetric) flow rate to volume ratio ($\frac{\Phi}{V_l}$) as summarized in Tables S1-S4.

The concentration decays due to a combination of first-order loss and gas-liquid equilibration, i.e., partitioning of PAN (or PPN) from the liquid reservoir to the gas stream. Kames and Schurath (1995) showed that under these conditions, the analyte's concentration decreases according to the following relationship:

$$-\frac{d}{dt}c_{\mathrm{g},t} = \left(\frac{\Phi}{H_S^{CC}V_l} + k_1\right)c_{\mathrm{g},t} \tag{5}$$

Here, $c_{g,t}$ is the analyte's concentration in the gas-phase at time t, k_l is the loss rate constant of PAN (or PPN) in the liquid phase, and H_S^{cccc} is the dimensionless Henry solubility. ~~Rearrangement~~ Integration of Eq. (5) yields:

$$\ln\left(\frac{c_{g,0}}{c_{g,t}}\right) = \left(\frac{\Phi}{H_S^{cccc} V_l} + k_l\right) t \qquad (6)$$

Since the chromatographic peak area (A) is proportional to c_g (Tokarek et al., 2014), linear regression analysis of plots of $\ln\left(\frac{A_{,0}}{A_{,t}}\right)$ versus $\frac{\Phi}{V_l}$ yields the values of $1/H_S^{cccc}$ as the slope and k_l as the intercept. In this work, peak areas were determined by fitting parameters of a Gaussian expression to the observed peaks as described by Tokarek et al. (2014) using an automated macro in Igor Pro (Wavemetrics Inc.).

The H and k_l constants measured in this work allow constraints to be placed on the heterogeneous uptake of the PANs. Under conditions of rapid gas/liquid equilibration, the ~~fraction ratio of a trace gas's concentration in the liquid phase ([X]ₗ) relative to its gas phase concentration ([X]g) is equal to~~

$$~~\frac{[X]_l}{[X]_g} = H_S^{cccc} \times L \qquad (7)~~$$

~~and its~~ first-order rate constant with respect to heterogeneous processing (k_{het}) is given by (Schwartz, 2003):

$$k_{het} = k_l \times H_S^{cccc} \times L. \qquad (\tilde{7}8)$$

Here, L is the ratio of the liquid volume divided by the total volume of an air parcel. The formulism of Eq. (7~~8~~) can be applied to liquid water (L_{aq} and $k_{l,aq}$) or organic aerosol (L_{org} and $k_{l,org}$). Hence, Eq. (~~8~~7) may be used to calculate the loss rate of a molecule with respect to wet deposition (k_{wet}) or organic aerosol uptake (k_{org}).

Another quantity that may be derived from knowledge of H and k_l constants is the reactive uptake probability (γ) for aqueous and (liquid) organic aerosol (Villalta et al., 1996):

$$\gamma \approx \frac{4 H_S^{cpcp} RT \sqrt{k_l D_l}}{\omega} = \frac{4 H_S^{cccc} \sqrt{k_l D_l}}{\omega}. \qquad (\tilde{9}8)$$

Here, ω is the mean molecular speed ($= \sqrt{\frac{8RT}{\pi M}}$ where M is the molecular weight, e.g., 0.1351 kg mol^{-1} for PPN), and D_l is the liquid phase diffusion coefficient (in m^2 s^{-1}), a quantity that can vary by many orders of magnitude depending on aerosol morphology (Shiraiwa et al., 2011). In this work, the magnitude of D_l was estimated using the semiempirical equation by Reddy and Doraiswamy (1967):

$$D_l \approx \psi \frac{M_l^{1/2} T}{\mu V_1^{1/3} V_2^{1/3}}. \qquad (\tilde{9}10)$$

185 Here, M_1 is the molecular weight of the solvent, μ is the solvent viscosity (in mPa s), V_1 and V_2 are the molar volumes of the solute and solvent (in $cm^3\,g^{-1}\,mol$), respectively, and ψ is a constant equal to 8.5×10^{-8} when $V_2/V_1>1.5$ and 10×10^{-8} when $V_2/V_1\leq1.5$ (Reddy and Doraiswamy, 1967).

Once a value of γ is ~~known~~estimated, the rate constant with respect to heterogeneous uptake in the kinetic limit (i.e., for submicron-sized aerosol) is then given by

190
$$k_{\text{het}} = \tfrac{1}{4}\omega\,\gamma\,S_A \tag{10}$$

where S_A is the specific surface area density of the aerosol (Davidovits et al., 2006).

RESULTS

Five consecutive chromatograms from a sample experiment are shown in Figure 2. In this example, the
195 bubble column apparatus was filled with 150 mL of DI water at a temperature of 5.00 °C which was equilibrated with PPN. The dominant peak in the chromatogram is PPN, eluting at ~288 s. The peak eluting at ~87 s (whose area is ~5% that of PPN) is due to ethyl nitrate (EN), a by-product of the PPN synthesis (Williams et al., 2000). There was also a small peak at ~136.5 s corresponding to PAN, another (though very minor) by-product of PPN synthesis. The relative elution times of EN, PAN, and PPN are consistent
200 with their capacity factors of medium polarity columns (Roberts et al., 1989).

The chromatograms show a decrease in gas-phase concentrations over time as humidified N_2 is bubbled through the water column at a volumetric flow rate of 238 mL min^{-1}. Representative plots of $\ln\left(\frac{c_{\text{g,0}}}{c_{\text{g,}t}}\right)$ versus t for PPN in DI water are shown in Figure 3. The subset of the data plotted in Figure 2 are highlighted in bold and red colour. Example plots of $\ln\left(\frac{c_{\text{g,0}}}{c_{\text{g,}t}}\right)$ versus t for PPN in n-octanol are shown in the S.I. as Figure
205 S1. Plots such as those shown in Figures 3 and S1 were linear with Pearson correlation coefficients (r) > 0.99 for all experiments. Experiments with PPN in n-octanol usually required more time than those with DI water to equilibrate initially (as judged by initial deviation from linearity of plots of $\ln\left(\frac{c_{\text{g,0}}}{c_{\text{g,}t}}\right)$ versus t). Because of the much slower decay rate, however, samples lasted for up to three days and allowed several flow conditions (i.e., different values of $\frac{\Phi}{V_l}$) to be probed in a single experiment.

210 Sample plots of $\frac{\text{d}}{\text{d}t}\ln\left(\frac{c_{\text{g,0}}}{c_{\text{g,}t}}\right)$ versus $\frac{\Phi}{V_l}$ (viz. Eq. (6)) for experiments with PAN and PPN in DI water at temperatures of 20 °C, 12.5 °C and 5.0 °C are shown in Figure 4. The error bars shown here and in the remaining Figures as well as the uncertainties stated in all Tables are at the 1σ precision level. Analogous

plots for experiments with PPN in n-octanol are shown in the S.I. as Figure S2. Linear regression analysis yielded slopes equal to $1/H_S^{CCcc}$ (Tables S5-S7), from which H was calculated using Eq. (1). The results are summarized in Table 1, alongside available literature values.

Figure 5 graphically summarizes the H constants measured in this work, along with available literature data, including estimates from the GROup contribution Method for Henry's law Estimate (GROMHE) structure-activity relationship model (Raventos-Duran et al., 2010). The data are presented as Van't Hoff plots, i.e., by plotting H on a logarithmic scale versus $1000/T$ (with T in Kelvin). Fits of Eq. (3) in Igor Pro to the data shown in Figure 5 yielded C_H terms whose $\pm 1\sigma$ uncertainty encompassed zero, such that the C_H term was set to zero in subsequent fits. The results, i.e., values for A_H and B_H derived from Eq. (3) and linear fits to the data, are shown as solid lines in Figure 5 and are summarized in Table 2. Fits to literature values are shown as dashed lines.

Our measurements of H for PAN in DI water are in good agreement with the majority of the available literature. Because of this, we combined our data with those of Kames and Schurath (1995) to yield the expression $\ln(H_S^{CPcp}(\text{PAN})_{aq}/[\text{M atm}^{-1}]) = -(17.8\pm0.3) + (5620\pm85)/T$ where T is in Kelvin (Table 2). For PPN in DI water, on the other hand, our H data are systematically lower than those by Kames and Schurath (1995) and are best described by the expression $\ln(H_S^{CcpP}(\text{PPN})_{aq}/[\text{M atm}^{-1}]) = -(19.5\pm1.7) + (5955\pm480)/T$ (Table 2).

Henry's law constants for PPN in n-octanol ranged from (88 ± 5) M atm^{-1} at 25.0 °C to (204 ± 16) M atm^{-1} at 5.0 °C and were larger than those of PAN in n-octanol (Figure 5). The data are best described by the expression $\ln(H_S^{CPcp}(\text{PPN})_{oct}/[\text{M atm}^{-1}]) = -(6.92\pm0.75) + (3390\pm320)/T$ (Table 2). The H constants of both compounds exhibit similar temperature dependence with $\Delta H_{sol}^0 (\text{PAN})_{oct} \approx -(33\pm2)$ kJ mol^{-1} and $\Delta H_{sol}^0 (\text{PPN})_{oct} \approx -(28\pm3)$ kJ mol^{-1} (Table 2).

Using the measured H constants for PPN in DI water and n-octanol and Eq. (4), values of K_{OW} of PPN were calculated. The octanol-water partition coefficient of PPN ranges from 59 ± 4 at 25 °C to 29 ± 3 at 5 °C, a factor of $\sim(4.1\pm0.6)$ larger than those reported by Roberts (2005) for PAN (Table 3).

Loss rate constants determined from the intercepts of plots such as those shown in Figure 4 are summarized in Table 4. Values for $\ln(k_l/[\text{s}^{-1}])$ are plotted versus $1000/T$ in Figure 6 alongside literature values, including data extracted from Figure 7 of Kames and Schurath (1995) and the rate constants for thermal dissociation of PAN and PPN (Kabir et al., 2014). All k_l values in DI water are larger than (whereas all k_l values in n-octanol are smaller than) the thermal decomposition rates of PAN and PPN (Figure 6). Table 5 summarizes linear regression parameters to the data shown in Figure 6, i.e., the temperature dependence of k_l. The loss rate constant of PPN in n-octanol increases when a small amount of a radical scavenger, α-tocopherol (Niki

245 and Noguchi, 2004), is added to the solution (Figure S3) but is still smaller than PPN's thermal decomposition rate constant in the gas-phase as well as its loss rate constant in DI water (Table S8).

The results of this work allow constraints to be placed on the uptake of PPN by aqueous and organic matter in the atmosphere. The liquid water content (LWC or L_{aq}) of the atmosphere is highly variable and ranges from $<3\times10^{-6}$ g m^{-3} in the cloud-free atmosphere under low aerosol loading (Nenes et al., 2021) to >3 g m^{-3}

250 in cumulonimbus clouds in the Tropics (Rosenfeld and Lensky, 1998). Using values of $k_{l,aq}$ and $H_{S,aq}^{cccc}$ measured in this work and Eq. (7)8, we calculated the lifetimes with respect to hydrolysis ($\tau_{wet} = k_{wet}^{-1}$) of PAN and PPN for a range of atmospheric conditions including high (inorganic) aerosol loadings, clouds, and fog at 293 K (Table S9) and 278 K (Table S10). The calculated wet deposition lifetimes of PPN (and PAN) vary from several days (e.g., in the presence of marine fog) to years.

255 Reactive uptake probabilities calculated using Eq. (98) are summarized in Table S11. For DI water, γ values are on the order of ~10^{-6} for both PAN and PPN at 278 K and 293 K. For n-octanol, γ values are larger, varying between 4×10^{-6} (at 278 K) and 2×10^{-6} (293 K) for PAN and between 0.7×10^{-5} (278 K) and 1.1×10^{-5} (293 K) for PPN.

260 **DISCUSSION**

Solubility of PAN and PPN in DI water. The H data observed in this work for PAN (Figure 5, blue color) are in excellent agreement with the majority of the recent literature (Kames and Schurath, 1995; Kames et al., 1991; Frenzel et al., 2000; Lee, 1984) which gives confidence in the accuracy of the measurements presented in this manuscript. The only outlier is the data point by Holdren (1984) which is inconsistent with

265 all other measurements and appears to be in error. On the other hand, the H constants of PPN in DI water observed in this work (Figure 5, red color) are systematically smaller than those by Kames and Schurath (1995), the only other study of water solubility of PPN. At 293.15 K, for example, a value of $H_{aq} = (2.67\pm0.18)$ M atm^{-1} was observed in this work, ~8% lower than the literature value of (2.90 ± 0.06) M atm^{-1}. The gap widens at lower temperatures, e.g., to ~17% at 278.15 K. is larger (~17%) when H_S^{cp} values are

270 calculated based on the parameters in Table 2. The reason (or reasons) for this difference and whose measurement is ultimately more accurate are uncertain, though the results in this work are corroborated by the excellent agreement for PAN with literature (Figure 5).

The k_l values for PAN and PPN in DI water (Figure 6) are also consistent with literature values: They are smaller than those reported for PAN by Kames et al. (1991) and marginally larger than the values reported

275 for PAN and PPN by Kames and Schurath (1995). In DI water, all measured k_l constants are larger than the

thermal dissociation rates of either PAN or PPN (shown as dashed lines in Figure 6), consistent with the hydrolysis mechanism hypothesized by Kames et al. (1991).

In general, accurate measurements of k_l in unbuffered, DI water are challenging because the hydrolysis rate constants are larger in the presence of salts (Kames and Schurath, 1995) and pH dependent, i.e., base catalyzed (Lee, 1984) and slower in acidic solutions (Frenzel et al., 2000). Hence, impurities may potentially bias experimental data for unbuffered, DI water. The largest source of impurities is the sample loading stage because gas streams containing PAN or PPN in high purity are challenging to generate. A contributing factor for the observed differences for PPN between this work and the study of Kames and Schurath (1995) may thus have been the method of PPN generation: In this work, a diffusion source was used, whereas Kames and Schurath (1995) used a photochemical source based on 3-pentanone photolysis in the presence of NO_2 to generate PPN in situ. Both of these types of sources co-emit water-soluble impurities. It is clear that EN was emitted in this work, though only in minute quantities (Figure 2) that in all likelihood did not affect the solubility of PPN. In contrast, the photochemical source used by Kames and Schurath (1995) likely co-emitted, as they put it, "rather high mixing ratios" (~3000 ppmv) of 3-pentanone and would have also co-emitted a myriad of water-soluble photochemical by-products such as hydroperoxides, aldehydes and α,β-dicarbonyls such as glyoxal (Rider et al., 2015). Furthermore, formation of photochemical side products would have been accentuated in their work since they utilized a 254 nm Hg lamp whose high operating temperature heightens undesired secondary photochemistry (Rider et al., 2015). It is unclear whether these impurities would have altered the bulk properties of the water contained in their bubble column and hence led to different H and k_l values, but it is certainly conceivable. Both diffusion and photochemical sources may have also co-emitted some NO_2 generated from thermal decomposition of PAN or PPN, whose presence can increase the effective lifetime of PANs with respect to the thermal dissociation (Sehested et al., 1998), though fortunately this compound is many orders of magnitude less water-soluble than either PAN or PPN (Sander, 2015) such that the potential presence of NO_2 is inconsequential.

Solubility of PAN and PPN in n-octanol and K_{OW} values. This work represents, to the best of our knowledge, the first and only measurement of the solubility of PPN in an organic liquid and the first determination of K_{OW} for this compound.

The measured H_{oct} and K_{OW} constants are a factor of ~2.4±0.3 and ~4.1±0.6 larger for PPN than those reported by Roberts (2005) for PAN (Tables 1 and 3). These ratios are, qualitatively, rationalized by PPN's longer aliphatic side chain and are of similar relative magnitude as the K_{OW} constants reported by MacKay et al (2006) for ethyl and methyl acetate (5.4:1.5 ≈ 3.6) as well as ethyl and methyl formate (2.13:1.07 ≈ 2.0), i.e., the results are reasonable.

Wang et al. (2017) predicted gas-water and gas-organic partitioning coefficients for PAN and PPN using three independent prediction methods; however, their predicted values diverged considerably between each

310   other and differed by several orders of magnitude from the experimental values reported in this work, especially for air-water partitioning. This is broadly consistent with the conclusions of their paper that noted challenges of theoretical methods to accurately predict Henry's law constants, particularly for multifunctional compounds such as PAN or PPN.

The k_1 values measured for PPN in n-octanol (Figure 6) are consistent with (but more precise than) those

315   observed by Roberts (2005) for PAN and much smaller than the gas-phase thermal dissociation rate constants at all temperatures. The lower k_1 value is, qualitatively, rationalized by a solvent or "cage" effect, where PPN and PAN dissociate but the relative ~~lipophilic~~ lipophobic fragments recombine faster than they react. When a known radical scavenger, α-tocopherol, was added, k_1 increased but remained below the thermal dissociation limit (Figure S3 and Table S8), consistent with this interpretation.

320   **Atmospheric implications.** The results of this work allow constraints to be placed on the heterogeneous uptake of PPN in the atmosphere.

The calculated wet deposition lifetimes of PPN (and PAN) ~~have units~~are on the order of years (Tables S9 and S10), substantiating the conclusion by Kames and Schurath (1995) and others that wet deposition of these molecules in the troposphere is generally too slow to matter. The only potential exception is the

325   marine environment where the phase ratio ~~of [X]$_{aq}$:[X]$_g$~~ (~~Eq. (7)~~H_S^{cc}(PAN) × L; Tables S9 and S10) is large and can exceed 10^{-4} for both PAN and PPN and because Kames and Schurath (1995) measured a loss rate constant of 4.4×10^{-3} s^{-1} for filtered sea water, a factor of ~24 larger than that for DI water. The reason(s) for the larger k_1 values is (are) not known but suggests the presence of one (or more) reaction pathway(s) in addition to hydrolysis. Assuming this larger k_1 value for marine boundary layer (MBL) fog or cloud droplets,

330   τ_{wet} is on the order of tens of days for PPN and approximately half that for PAN (Tables S9 and S10). This suggests that wet deposition may potentially have contributed to the enhancement of the PPN:PAN ratio observed in the Gulf of Maine (Roberts et al., 1996). However, under the conditions of drizzling MBL fog as observed during the New England Air Quality Study (NEAQS) in 2004, the suspended droplets would more likely resemble pure water droplets as opposed to droplets resembling oceanic surface water, which

335   in turn would imply hydrolysis lifetimes on the order of hundreds of days and a negligible loss by wet deposition.

This work has shown that the H constants of PPN in n-octanol are larger than those for PAN ~~n~~ in n-octanol, which suggests that PPN will be more soluble in organic aerosol (OA). Assuming $L_{org}=5\times10^{-11}$ (Roberts, 2005) and further assuming that n-octanol is a good proxy of OA, we calculate ~~(using Eq. (7))~~ an

340   equilibrium fraction between 2×10^{-7} at 5 °C and 1×10^{-7} at 25 °C for the partitioning of PPN on OA,

Page 12

approximately double that of PAN but still orders of magnitude too small to be of consequence on the gas-phase concentration of PPN. For example, assuming an aerosol surface area characteristic of the polluted lower troposphere of $S_A = 1000$ μm^2 cm^{-3} and 50% (liquid) organic aerosol content and using $\gamma = 1\times10^{-5}$ estimated in this work for OA at 293 K (Table S11), the first-order rate constant of PPN uptake (k_{org}) would be ~3×10^{-7} s^{-1}, or a lifetime of ~43 days, which is negligible. Further, the viscosity of OA is often larger than assumed for the calculations in Table S11, i.e., D_l can be many orders of magnitude smaller than 10^{-9} m^2 s^{-1} (Shiraiwa et al., 2011). On the other hand, uptake of a radical precursor such as PPN on OA may very well initiate secondary radical chemistry within the particle phase that is believed to yield oligomeric and humic-like substances (Lim et al., 2010), which in turn suggests that uptake of PPN should not be ignored.

Our work provides the first estimates of γ values for PPN (Table S11) since there are, to the best of our knowledge, no experimental measurements of γ for PPN in the open literature. However, our γ estimates for PAN are at odds with a recent publication by Sun et al. (2022) who reported γ values in the range of (6 - 9)$\times10^{-5}$ for ambient aerosol at high relative humidity (RH) which are substantially larger than those calculated for DI water in this work (~10^{-6}; Table S11). They argued that the large uptake on ambient aerosol would be driven by chemical loss of PAN within the particle phase via unspecified redox reactions, yielding a substantially larger k_l, which is reminiscent of the observation by Kames and Schurath (1995) for filtered sea water. However, because the uptake of PAN scales with $\sqrt{k_l}$, a factor of ~15 larger uptake in turn would require a ~200× larger liquid-phase reaction rate constant, which seems unrealistic or would require some currently unknown chemistry.

Data availability

The $\frac{\mathrm{d}}{\mathrm{dt}}\ln\left(\frac{c_{g,o}}{c_{g,t}}\right)$ and associated T and $\frac{\varPhi}{V_l}$ data for the experiments discussed are tabulated in the S.I. Raw data (i.e., digitized chromatograms) have been placed in an online repository, accessible at https://doi.org/10.5683/SP3/IYXA3G, and are also available from the corresponding author upon request (hosthoff@ucalgary.ca) upon request.

Author contributions

MAV (PPN in water using the Varian GC-ECD), KDE (PPN in n-octanol using the Varian GC-ECD), KNA (PAN in water using the HP GC-ECD), and AMM (PAN in water using the Varian GC-ECD) carried out the experiments and reduced the data. MAV and KNA synthesized PPN and PAN, respectively. HDO conceptualized the experiments and drafted the manuscript with input from KDE.

Competing interests

The authors declare that they have no conflict of interest.

375 **Acknowledgments**

This work was made possible by the financial support of the Natural Sciences and Engineering Research Council of Canada (NSERC) in the form of a Discovery grant to HDO (RGPIN/03849-2016). KDE acknowledges an NSERC undergraduate student research award (USRA).

380 **References**

Burkholder, J. B., Sander, S. P., Abbatt, J. P. D., Barker, J. R., Cappa, C., Crounse, J. D., Dibble, T. S., Huie, R. E., Kolb, C. E., Kurylo, M. J., Orkin, V. L., Percival, C. J., Wilmouth, D. M., and Wine, P. H.: Chemical Kinetics and Photochemical Data for Use in Atmospheric Studies, Evaluation Number 19, JPL Publication 19-5, National Aeronautics and Space Administration, Jet Propulsion Laboratory,
385 California Institute of Technology, Pasadena, California, 2020.

Davidovits, P., Kolb, C. E., Williams, L. R., Jayne, J. T., and Worsnop, D. R.: Mass accommodation and chemical reactions at gas-liquid interfaces, Chem. Rev., 106, 1323-1354, 10.1021/cr040366k, 2006.

Frenzel, A., Kutsuna, S., Takeuchi, K., and Ibusuki, T.: Solubility and reactivity of peroxyacetyl nitrate (PAN) in dilute aqueous salt solutions and in sulphuric acid, Atmos. Environm., 34, 3641-3644,
390 10.1016/S1352-2310(00)00132-1, 2000.

Furgeson, A., Mielke, L. H., Paul, D., and Osthoff, H. D.: A photochemical source of peroxypropionic and peroxyisobutanoic nitric anhydride, Atmos. Environm., 45, 5025-5032, 10.1016/j.atmosenv.2011.03.072, 2011.

Gaffney, J. S., and Marley, N. A.: The Impacts of Peroxyacetyl Nitrate in the Atmosphere of Megacities
395 and Large Urban Areas: A Historical Perspective, ACS Earth Space Chem., 10.1021/acsearthspacechem.1c00143, 2021.

Harwood, M. H., Roberts, J. M., Frost, G. J., Ravishankara, A. R., and Burkholder, J. B.: Photochemical studies of $CH_3C(O)OONO_2$ (PAN) and $CH_3CH_2C(O)OONO_2$ (PPN): NO_3 quantum yields, J. Phys. Chem. A, 107, 1148-1154, 10.1021/jp0264230, 2003.

400 Holdren, M. W., Spicer, C. W., and Hales, J. M.: Peroxyacetyl nitrate solubility and decomposition rate in acidic water, Atmos.Environm. (1967), 18, 1171-1173, 10.1016/0004-6981(84)90148-3, 1984.

Kabir, M., Jagiella, S., and Zabel, F.: Thermal Stability of n-Acyl Peroxynitrates, Internat. J. Chem. Kin., 46, 462-469, 10.1002/kin.20862, 2014.

Kames, J., Schweighoefer, S., and Schurath, U.: Henry's law constant and hydrolysis of peroxyacetyl
405 nitrate (PAN), J. Atmos. Chem., 12, 169-180, 10.1007/BF00115778, 1991.

Kames, J., and Schurath, U.: Henry's law and hydrolysis rate constants for peroxyacyl nitrates (PANs) using a homogeneous gas-phase source, J. Atmos. Chem., 21, 151-164, 10.1007/BF00696578, 1995.

Koracin, D., Lewis, J., Thompson, W. T., Dorman, C. E., and Businger, J. A.: Transition of stratus into fog along the California coast: Observations and modeling, Journal of the Atmospheric Sciences, 58,
410 1714-1731, 10.1175/1520-0469(2001)058<1714:Tosifa>2.0.Co;2, 2001.

Lee, Y. N.: Kinetics of some aqueous-phase reactions of peroxyacetyl nitrate, Brookhaven National Lab., Upton, NY (USA)BNL-34735; CONF-840489-4; ON:DE84011911, 1984.

Lim, Y. B., Tan, Y., Perri, M. J., Seitzinger, S. P., and Turpin, B. J.: Aqueous chemistry and its role in secondary organic aerosol (SOA) formation, Atmos. Chem. Phys., 10, 10521-10539, 10.5194/acp-10-10521-2010, 2010.

Mackay, D., Shiu, W. Y., Ma, K.-C., and Lee, S. C.: Handbook of physical-chemical properties and environmental fate for organic chemicals, 2nd ed., CRC/Taylor & Francis, Boca Raton, FL, 2006.

Mackay, D., and Parnis, J. M.: Multimedia environmental models : the fugacity approach, 3rd ed., Taylor & Francis, 2020.

McFadyen, G. G., and Cape, J. N.: Spring time sources and sinks of Peroxyacetyl Nitrate in the UK and its contribution to acidification and nitrification of cloud water, Atmospheric Research, 50, 359-371, 10.1016/s0169-8095(98)00102-1, 1999.

Mielke, L. H., and Osthoff, H. D.: On quantitative measurements of peroxycarboxylic nitric anhydride mixing ratios by thermal dissociation chemical ionization mass spectrometry, Int. J. Mass Spectrom., 310, 1-9, 10.1016/j.ijms.2011.10.005, 2012.

Mitchell, M.: Engauge Digitizer: doi: 10.5281/zenodo.3941227, 2021.

Nenes, A., Pandis, S. N., Kanakidou, M., Russell, A. G., Song, S., Vasilakos, P., and Weber, R. J.: Aerosol acidity and liquid water content regulate the dry deposition of inorganic reactive nitrogen, Atmos. Chem. Phys., 21, 6023-6033, 10.5194/acp-21-6023-2021, 2021.

Niki, E., and Noguchi, N.: Dynamics of Antioxidant Action of Vitamin E, Accounts of Chemical Research, 37, 45-51, 10.1021/ar030069m, 2004.

Raventos-Duran, T., Camredon, M., Valorso, R., Mouchel-Vallon, C., and Aumont, B.: Structure-activity relationships to estimate the effective Henry's law constants of organics of atmospheric interest, Atmos. Chem. Phys., 10, 7643-7654, 10.5194/acp-10-7643-2010, 2010.

Reddy, K. A., and Doraiswamy, L. K.: Estimating Liquid Diffusivity, Industrial & Engineering Chemistry Fundamentals, 6, 77-79, 10.1021/i160021a012, 1967.

Rider, N. D., Taha, Y. M., Odame-Ankrah, C. A., Huo, J. A., Tokarek, T. W., Cairns, E., Moussa, S. G., Liggio, J., and Osthoff, H. D.: Efficient photochemical generation of peroxycarboxylic nitric anhydrides with ultraviolet light-emitting diodes, Atmos. Meas. Tech., 8, 2737-2748, 10.5194/amt-8-2737-2015, 2015.

Roberts, J. M., Fajer, R. W., and Springston, S. R.: Capillary gas chromatographic separation of alkyl nitrates and peroxycarboxylic nitric anhydrides, Anal. Chem., 61, 771-772, 10.1021/ac00182a026, 1989.

Roberts, J. M.: The atmospheric chemistry of organic nitrates, Atmos. Environm. A, 24, 243-287, 10.1016/0960-1686(90)90108-Y, 1990.

Roberts, J. M., Parrish, D. D., Norton, R. B., Bertman, S. B., Holloway, J. S., Trainer, M., Fehsenfeld, F. C., Carroll, M. A., Albercook, G. M., Wang, T., and Forbes, G.: Episodic removal of NO_y species from the marine boundary layer over the North Atlantic, J. Geophys. Res.-Atmos., 101, 28947-28960, 10.1029/96jd02632, 1996.

450 Roberts, J. M.: Measurement of the Henry's law coefficient and first order loss rate of PAN in n-octanol, Geophys. Res. Lett., 32, L08803, 10.1029/2004gl022327, 2005.

Roberts, J. M.: PAN and Related Compounds, in: Volatile Organic Compounds in the Atmosphere, edited by: Koppmann, R., Blackwell Publishing, Oxford, UK, 221-268, 2007.

Roberts, J. M., Marchewka, M., Bertman, S. B., Sommariva, R., Warneke, C., de Gouw, J., Kuster, W.,

455 Goldan, P., Williams, E., Lerner, B. M., Murphy, P., and Fehsenfeld, F. C.: Measurements of PANs during the New England Air Quality Study 2002, J. Geophys. Res., 112, D20306, 10.1029/2007jd008667, 2007.

Rosenfeld, D., and Lensky, I. M.: Satellite-Based Insights into Precipitation Formation Processes in Continental and Maritime Convective Clouds, Bulletin of the American Meteorological Society, 79,

460 2457-2476, 10.1175/1520-0477(1998)079<2457:Sbiipf>2.0.Co;2, 1998.

Sander, R.: Compilation of Henry's law constants (version 4.0) for water as solvent, Atmos. Chem. Phys., 15, 4399-4981, 10.5194/acp-15-4399-2015, 2015.

Sander, R., Acree, W. E., Visscher, A. D., Schwartz, S. E., and Wallington, T. J.: Henry's law constants (IUPAC Recommendations 2021), Pure Appl. Chem., 94, 71-85, 10.1515/pac-2020-0302, 2022.

465 Schwartz, S.: Presentation of solubility data: Units and applications, in: Chemicals in the atmosphere: solubility, sources, and reactivity, edited by: Fogg, P. G. T., and Sangster, J., 7, J. Wiley, Hoboken, NJ, 453, 2003.

Sehested, J., Christensen, L. K., Mogelberg, T., Nielsen, O. J., Wallington, T. J., Guschin, A., Orlando, J. J., and Tyndall, G. S.: Absolute and relative rate constants for the reactions $CH_3C(O)O_2+NO$ and

470 $CH_3C(O)O_2+NO_2$ and thermal stability of $CH_3C(O)O_2NO_2$, J. Phys. Chem. A, 102, 1779-1789, 10.1021/jp972881a, 1998.

Shiraiwa, M., Ammann, M., Koop, T., and Poschl, U.: Gas uptake and chemical aging of semisolid organic aerosol particles, Proc. Natl. Acad. Sci., 108, 11003-11008, 10.1073/pnas.1103045108, 2011.

Sparks, J. P., Roberts, J. M., and Monson, R. K.: The uptake of gaseous organic nitrogen by leaves: A

475 significant global nitrogen transfer process, Geophys. Res. Lett., 30, 2189, 10.1029/2003gl018578, 2003.

Staudinger, J., and Roberts, P. V.: A critical compilation of Henry's law constant temperature dependence relations for organic compounds in dilute aqueous solutions, Chemosphere, 44, 561-576, 10.1016/S0045-6535(00)00505-1, 2001.

480 Sun, M., Zhou, Y., Wang, Y., Qiao, X., Wang, J., and Zhang, J.: Heterogeneous Reaction of Peroxyacetyl
Nitrate on Real-World PM2.5 Aerosols: Kinetics, Influencing Factors, and Atmospheric Implications,
Environm. Sci. Technol., 56, 9325-9334, 10.1021/acs.est.2c03050, 2022.

Talukdar, R. K., Burkholder, J. B., Schmoltner, A. M., Roberts, J. M., Wilson, R. R., and Ravishankara,
A. R.: Investigation of the loss processess for peroxyacetyl nitrate in the atmosphere - UV Photolysis
485 and reaction with OH, J. Geophys. Res., 100, 14163-14173, 10.1029/95JD00545, 1995.

Teklemariam, T. A., and Sparks, J. P.: Gaseous fluxes of peroxyacetyl nitrate (PAN) into plant leaves,
Plant Cell and Environment, 27, 1149-1158, 2004.

Tokarek, T. W., Huo, J. A., Odame-Ankrah, C. A., Hammoud, D., Taha, Y. M., and Osthoff, H. D.: A gas
chromatograph for quantification of peroxycarboxylic nitric anhydrides calibrated by thermal
490 dissociation cavity ring-down spectroscopy, Atmos. Meas. Tech., 7, 3263-3283, 10.5194/amt-7-3263-
2014, 2014.

Villalta, P. W., Lovejoy, E. R., and Hanson, D. R.: Reaction probability of peroxyacetyl radical on
aqueous surfaces, Geophys. Res. Lett., 23, 1765-1768, 10.1029/96GL01286, 1996.

Wang, C., Yuan, T., Wood, S. A., Goss, K. U., Li, J., Ying, Q., and Wania, F.: Uncertain Henry's law
495 constants compromise equilibrium partitioning calculations of atmospheric oxidation products, Atmos.
Chem. Phys., 17, 7529-7540, 10.5194/acp-17-7529-2017, 2017.

Williams, J., Roberts, J. M., Fehsenfeld, F. C., Bertman, S. B., Buhr, M. P., Goldan, P. D., Hubler, G.,
Kuster, W. C., Ryerson, T. B., Trainer, M., and Young, V.: Regional ozone from biogenic
hydrocarbons deduced from airborne measurements of PAN, PPN, and MPAN, Geophys. Res. Lett.,
500 24, 1099-1102, 10.1029/97GL00548, 1997.

Williams, J., Roberts, J. M., Bertman, S. B., Stroud, C. A., Fehsenfeld, F. C., Baumann, K., Buhr, M. P.,
Knapp, K., Murphy, P. C., Nowick, M., and Williams, E. J.: A method for the airborne measurement
of PAN, PPN, and MPAN, J. Geophys. Res., 105, 28943-28960, 10.1029/2000JD900373, 2000.

Zborowska, A. G., MacInnis, C. Y., Ye, C. Z., and Osthoff, H. D.: On the photolysis branching ratio of
505 methyl ethyl ketone, Atmos. Environm., 254, 118383, 10.1016/j.atmosenv.2021.118383, 2021.
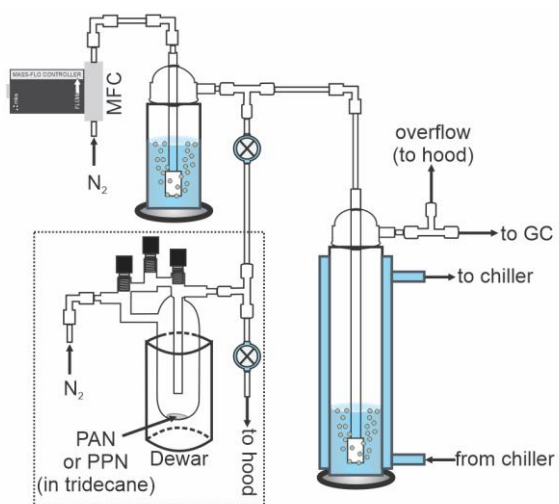
Figure 1. Schematic of the experimental apparatus (not to scale). The dashed line encompasses the PAN (or PPN) diffusion source; MFC = mass flow controller. The bubbler shown in the top left was removed for experiments with n-octanol.
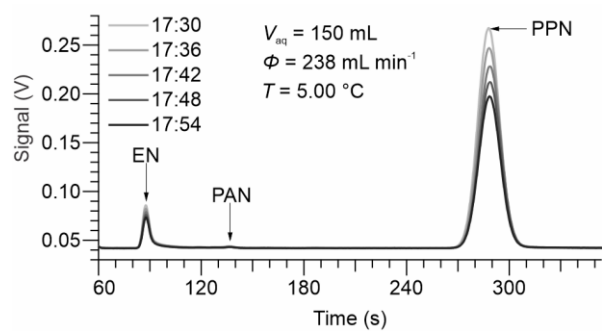
Figure 2. Sample chromatograms recorded by the Varian GC-ECD operated with N_2 carrier gas at a flow rate of 40 mL min^{-1}. Here, the GC sampled the gas eluting from 150 mL DI water at a temperature of 5.00 °C at a volumetric flow rate of 238 mL min^{-1}. The GC injected automatically every 360 s, at the time (in HH:MM) shown in the legend.
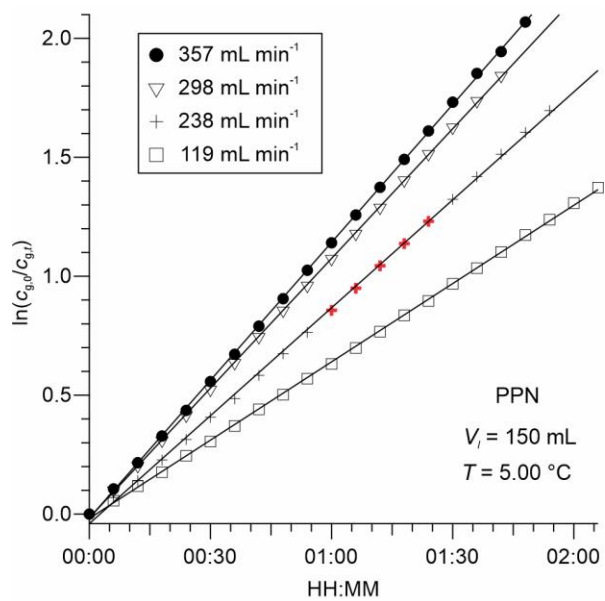
Figure 3. Plots of $\ln(c_{g,0}/c_{g,t})$ for PPN versus t, observed downstream from 150 mL of DI water at 5.00 °C for four different volumetric flow rates. The data from Figure 2 are highlighted in bold and red colour.
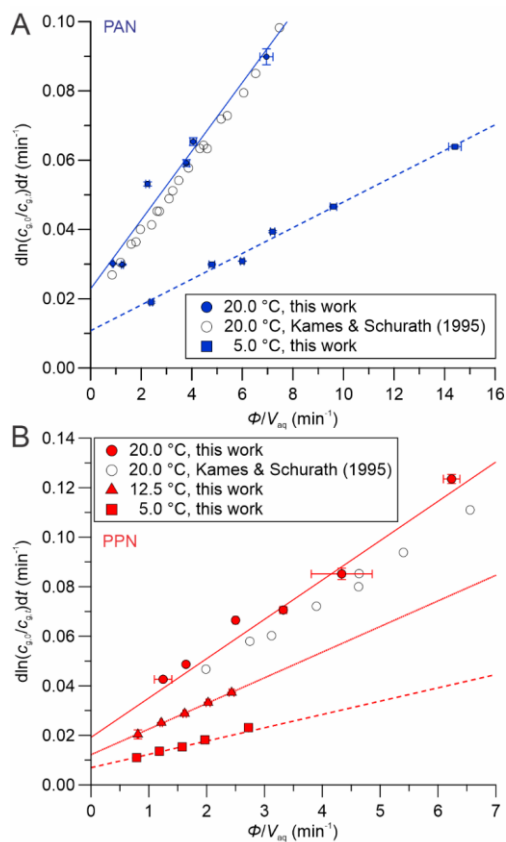
520

Figure 4. (A) Plots of $dln(c_{g,0}/c_{g,t})/dt$ versus Φ/V_l for PAN in DI water at 20.0 °C (●) and 5.0 °C (■). Literature data at 20.0 °C were extracted from Figures 4 and 5 of Kames and Schurath (1995) using "Engauge Digitizer" software (Mitchell, 2021) and are shown as open symbols (○). The lines are linear fits to the data at each temperature. **(B)** Same plot as panel (A) but for PPN in DI water and also showing data

525 at 12.5 °C (▲).
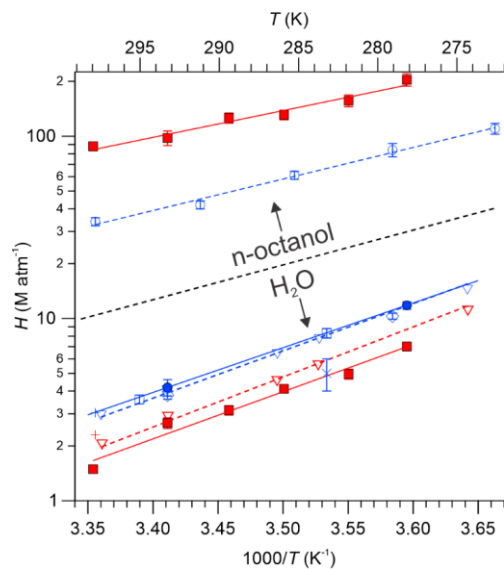
Figure 5. Henry's law constants for PAN (blue color) and PPN (red color) ~~for~~ in n-octanol and DI water as functions of temperature. Data from this work are shown as solid symbols (● for PAN and ■ for PPN). Data from Figure 6 of Kames and Schurath (1995) for PAN and PPN were extracted using "Engauge Digitizer" software (Mitchell, 2021) and are shown as ▽ and ⁻⁻. Other literature data are shown as follows: □ (Lee, 1984). × (Holdren et al., 1984). △ (Kames et al., 1991). ◇ (Frenzel et al., 2000). ○ and ⁻⁻ (Roberts, 2005). + (Raventos-Duran et al., 2010). The dashed, black line serves as a visual indicator to separate results obtained with n-octanol (top portion of graph) from those obtained with DI water (bottom).
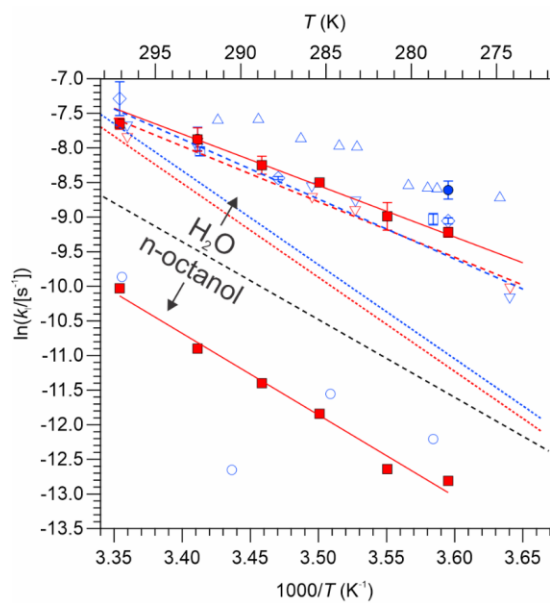
535

Figure 6. Natural logarithm of k_1 of PAN (blue color) and PPN (red color) in DI water and n-octanol plotted versus $1000/T$. Data from this work are shown as solid symbols (● for PAN and ■ for PPN). Literature data: × (Holdren et al., 1984). △ (Kames et al., 1991). ▽-- (Kames and Schurath, 1995). ◇ (Frenzel et al., 2000). ○ (Roberts, 2005). Error bars for the data by Roberts (2005) are omitted for clarity. The dashed blue and

540 red lines ("") are the expressions by Kabir et al. (2014) for thermal dissociation of PAN and PPN, respectively. The dashed, black line serves as a visual indicator to separate results obtained with n-octanol (bottom portion of graph) from those obtained with DI water (top).

Table 1. Summary of Henry's law solubility constants. N/A = not available (not tabulated). n/d = not determined.

Compound and solvent	Reference	H_S^{CPcp} (M atm^{-1})					
		298.15 K	293.15 K	289.15 K	285.65 K	281.65 K	278.15 K
PAN in DI water	(Lee, 1984)	n/d	3.6±0.2 (295 K)	n/d	8.3±0.5 (283 K)	n/d	n/d
	(Holdren et al., 1984)	n/d	n/d	n/d	5±1 (283 K)	n/d	n/d
	(Kames et al., 1991)	N/A	4.10±0.15	N/A	N/A	N/A	N/A
	(Kames and Schurath, 1995)	N/A	4.10±0.08	N/A	N/A	N/A	N/A
	(Frenzel et al., 2000)	n/d	3.8±0.2	n/d	n/d	n/d	10.3±0.4 (279 K)
	(Burkholder et al., 2020)[*]	2.9[*]	4.0[*]	5.3[*]	6.7[*]	9.0[*]	11.6[*]
	(Raventos-Duran et al., 2010)[**]	3.04	n/d	n/d	n/d	n/d	n/d
	This work	n/d	4.2±0.4	n/d	n/d	n/d	11.8±0.6
PPN in DI water	(Kames and Schurath, 1995)	N/A	2.90±0.06	N/A	N/A	N/A	N/A
	(Raventos-Duran et al., 2010)[**]	2.30	n/d	n/d	n/d	n/d	n/d
	This work	1.49±0.05	2.67±0.18	3.14±0.19	4.11±0.07	4.96±0.31	7.01±0.25
PAN in n-octanol	(Roberts, 2005)	34±2	42±2 (291 K)	n/d	61±3 (285 K)	n/d	84±7 (279 K)

PPN in n-octanol	This work	88±5	98±9	126±8	131±8	157±11	204±16

* Literature evaluation with Uuncertainty factor of 2 to 10.

** Calculated based on structure-activity relationships.

Table 2. Temperature dependence of Henry's law solubility constants derived by linear fitting of Eq. (3) with C_H=0 to the data shown in Figure 5. n/d = not disclosed. N/A = not applicable.

Compound and solvent	Reference	r^2 (%)	$-B_H$ (10^3 K^{-1})	A_H (unitless)	$-R{\times}B_H = -\Delta H^0_{sol}$ (kJ mol^{-1})	$R{\times}A_H$ (J K^{-1} mol^{-1})
PAN in DI water	(Lee, 1984)[*]	n/d	5.9±0.6	-19±2	49.2±4.7	-157±16
	(Kames et al., 1991)	n/d	6.5±0.1	-20.8±0.5	54.2±1.0	-173.1±4
	(Kames and Schurath, 1995)	n/d	5.7±0.2	-18.0±0.6	47.4±1.6	-150±5
	(Burkholder et al., 2020)[**]	N/A	5.73	-18.15	47.6	-151
	This work[***]	99.89	5.62±0.09	-17.8±0.3	46.7±0.7	-148±3
PPN in DI water	(Kames and Schurath, 1995)	n/d	5.9±0.1	-19.2±0.4	49.4±0.9	-160±3
	This work	97.5	6.0±0.5	-19.5±1.7	49.5±4.0	-162±14
PAN in n-octanol	(Roberts, 2005)	99.1	4.0±0.2	-9.9±0.8	33.1±1.8	-82.1±6.3
PPN in n-octanol	This work	96.7	3.4±0.3	-6.9±0.8	28.2±2.6	-57.5±6.3

[*] Value for ΔS^0_{sol} and uncertainties were calculated by Kames and Schurath (1995) based on data provided by Lee (1984).

[**] Uncertainty factor of 2 to 10.

[***] Data from this work combined with those of (Kames and Schurath, 1995).

Table 3. n-Octanol - water partition coefficients of PAN and PPN calculated using Eq. (4). n/d = not determined.

Compound	Reference	298.15 K	293.15 K	289.15 K	285.65 K	281.65 K	278.15 K
PAN	(Roberts, 2005)	11.8±0.7	9.2±0.5 (291 K)	n/d	8.8±0.5 (285 K)	n/d	7.8±0.7 (279 K)
PPN	This work	59.1±3.8	36.6±4.2	40.1±3.5	31.8±2.0	31.6±3.0	29.1±2.5

560

Table 4. Summary of liquid-phase loss rate constants. N/A = not available (not tabulated). n/d = not determined.

Compound and solvent	Reference	k_l $(10^{-5}\ s^{-1})$					
		298.15 K	293.15 K	289.15 K	285.65 K	281.65 K	278.15 K
PAN in DI water	(Holdren et al., 1984)	n/d	68±17 (298 K)	n/d	21.7±0.5 (288 K)	n/d	11.7±0.5
	(Kames et al., 1991)		64±19	N/A	N/A	N/A	N/A
	(Kames and Schurath, 1995)		34±1	N/A	19[*]	N/A	N/A
	(Frenzel et al., 2000)		32±2	n/d	n/d	n/d	12±1 (279 K)
	This work		38±7	n/d	n/d	n/d	18±2
PPN in DI water	(Kames and Schurath, 1995)	N/A	31±2	N/A	17[*]	N/A	N/A
	This work	47±4	38±6	26±3	20.3±0.5	12±3	9.9±0.7
PAN in n-octanol	(Roberts, 2005)	5.2±1.9	0.32±0.25 (291 K)	n/d	0.96±1.8 (285 K)	n/d	0.5±2.6 (279 K)
PPN in n-octanol	This work	4.4±0.2	1.8±0.3	1.1±0.2	0.7±0.1	0.3±0.2	0.3±0.2

565   [*] Value estimated from Fig. 7 of (Kames and Schurath, 1995).

Table 5. Temperature dependence of liquid-phase loss rate constants.

Compound and solvent	Reference	E_a (kJ mol^{-1})	A (s^{-1})
PPN in DI water	(Kames and Schurath, 1995)	54.5±3.1	$10^{6.2\pm0.6}$
PPN in DI water	This work	57.0±3.4	$10^{6.7\pm0.6}$
PAN in n-octanol	(Roberts, 2005)	67±56	$10^{7.1\pm10.2}$
PPN on n-octanol	This work	97.5±6.2	$10^{12.7\pm1.1}$

Supplemental information for

Measurement of Henry's law and liquid-phase loss rate constants of peroxypropionic nitric anhydride (PPN) in deionized water and in n-octanol

Kevin D. Easterbrook,[1] Mitchell A. Vona,[1] Kiana Nayebi-Astaneh,[1] Amanda M. Miller,[1] and Hans D. Osthoff[1]

[1] Department of Chemistry, University of Calgary, 2500 University Drive N.W., Calgary, Alberta, Canada T2N 1N4

Correspondence to: Hans D. Osthoff (hosthoff@ucalgary.ca)

for *Atmos. Chem. Phys.*

Contents

Table S1. Schedule of experiments: PAN in DI water.

Internal reference	GC-ECD	T (°C)	V_l (mL)	Φ (mL min^{-1})	$\dfrac{\Phi}{V_l}$ (min^{-1})	$\dfrac{\mathrm{d}}{\mathrm{d}t}\ln\left(\dfrac{c_{g,0}}{c_{g,t}}\right)$ (min^{-1})
KN 211026	HP	20.0±0.1	140±2	317±3	2.26±0.04	0.0532±0.0006
KN 211028	HP	20.0±0.1	140±2	532±6	3.80±0.07	0.0592±0.0010
AM 211108	Varian	20.00±0.01	140±2	124±1	0.89±0.02	0.0302±0.0001
HO 211108	HP	5.0±0.1	100±2	240±3	2.40±0.05	0.0190±0.0003
AM 211116	Varian	5.00±0.01	50.0±0.4	481±5	9.6±0.1	0.0466±0.0001
KN 211118-1	HP	5.0±0.1	75.0±0.4	541±6	7.21±0.09	0.0394±0.0003
KN 211104	HP	5.0±0.1	30.0±0.4	433±5	14.4±0.2	0.0639±0.0004
KN 211116	HP	5.0±0.1	100±2	481±5	4.81±0.11	0.0299±0.0002
KN 211118-2	HP	20.0±0.1	140±2	177±2	1.27±0.02	0.0299±0.0002
KN 211123	HP	20.0±0.1	140±2	570±6	4.07±0.07	0.0654±0.0011
AM 211123	Varian	5.00±0.01	75.0±0.4	451±5	6.01±0.07	0.0309±0.0001
KN 211125	HP	20.0±0.1	100±2	697±8	6.97±0.16	0.0899±0.0023

Table S2. Schedule of experiments: PPN in DI water. Experiments were conducted with the Varian GC-ECD.

Internal reference	T (°C)	V_l (mL)	Φ (mL min^{-1})	$\dfrac{\Phi}{V_l}$ (min^{-1})	$\dfrac{\mathrm{d}}{\mathrm{d}t}\ln\left(\dfrac{c_{g,0}}{c_{g,t}}\right)$ (min^{-1})
MV 220301	20.00±0.01	100±2	125±15	1.25±0.15	0.043±0.005
MV 220308	20.00±0.01	100±2	433±52	4.33±0.53	0.085±0.002
MV 220315-1	20.00±0.01	150±2	496±5	3.33±0.06	0.0706±0.0010
MV 220315-2	20.00±0.01	100±2	620±7	6.23±0.14	0.1235±0.0018
MV 220317-1	5.00±0.01	150±2	118±1	0.79±0.01	0.01098±0.00004
MV 220317-2	5.00±0.01	150±2	294±3	1.97±0.03	0.01818±0.00005
MV 220322-1	5.00±0.01	150±2	235±3	1.58±0.02	0.01533±0.00005
MV 220322-2	5.00±0.01	150±2	353±4	2.37±0.04	0.01932±0.00005
MV 220324-1	5.00±0.01	150±2	176±2	1.18±0.02	0.01357±0.00002

Table S2 (continued). Schedule of experiments: PPN in DI water. Experiments were conducted with the Varian GC-ECD.

Internal reference	T (°C)	V_l (mL)	Φ (mL min^{-1})	$\dfrac{\Phi}{V_l}$ (min^{-1})	$\dfrac{\mathrm{d}}{\mathrm{d}t}\ln\left(\dfrac{c_{g,0}}{c_{g,t}}\right)$ (min^{-1})
MV 220324-2	12.50±0.01	150±2	121±1	0.81±0.01	0.0204±0.00018
MV 220329-1	12.50±0.01	150±2	243±3	1.62±0.03	0.0288±0.0001
MV 220329-2	12.50±0.01	150±2	365±4	2.43±0.04	0.0373±0.0001
MV 220331-1	12.50±0.01	150±2	182±2	1.22±0.02	0.0251±0.0001
MV ~~220321~~220331-2	12.50±0.01	150±2	304±3	2.03±0.04	0.0332±0.0002
MV 220405-1	20.00±0.01	150±2	375±4	2.50±0.04	0.0665±0.0001
MV 220405-2	8.50±0.01	150±2	240±3	1.60±0.03	0.0212±0.0001
MV 220405-3	8.50±0.01	150±2	481±5	3.20±0.06	0.0345±0.0001
MV 220407-1	8.50±0.01	150±2	353±4	2.35±0.04	0.0285±0.0001
MV 220407-2	8.50±0.01	150±2	530±6	3.54±0.06	0.0388±0.0002
MV 220407-3	5.00±0.01	150±2	408±4	2.72±0.05	0.0231±0.0001
HO 220411-1	16.00±0.01	150±2	430±5	2.87±0.05	0.0567±0.0003
HO 220411-2	16.00±0.01	150±2	246±3	1.64±0.03	0.03744±0.00004
HO 220412-1	16.00±0.01	150±2	213±2	1.42±0.02	0.03453±0.00005
HO 220412-3	20.00±0.01	150±2	246±3	1.64±0.03	0.0487±0.0001
HO 220414-1	16.00±0.01	150±2	336±4	2.24±0.04	0.0451±0.0001
HO 220414-2	16.00±0.01	150±2	580±6	3.87±0.07	0.0665±0.0001
KE 220531-1	25.00±0.01	100.0±0.4	312±3	3.12±0.04	0.1122±0.0006
KE 220531-2	25.00±0.01	100.0±0.4	125±1	1.25±0.01	0.0628±0.0001
KE 220531-3	25.00±0.01	100.0±0.4	281±3	2.81±0.03	0.1048±0.0006
KE 220531-4	25.00±0.01	100.0±0.4	344±4	3.44±0.04	0.125±0.002
KE 220603-1	25.00±0.01	100.0±0.4	189±2	1.89±0.02	0.0810±0.0003

Table S3. Schedule of experiments: PPN in n-octanol. Experiments were conducted with the Varian GC-ECD.

Internal reference	T (°C)	V_l (mL)	Φ (mL min^{-1})	$\dfrac{\Phi}{V_l}$ (min^{-1})	$\dfrac{d}{dt}\ln\left(\dfrac{c_{g,0}}{c_{g,t}}\right)$ (min^{-1})
KE 220607-1c	20.00±0.01	50.0±0.4	277±3	5.54±0.08	0.00255±0.00004
KE 220607-1d	20.00±0.01	50.0±0.4	339±4	6.78±0.09	0.00381±0.00003
KE 220609-1b	20.00±0.01	50.0±0.4	186±2	3.73±0.05	0.00242±0.00005
KE 220609-1c	20.00±0.01	50.0±0.4	373±4	7.46±0.10	0.00413±0.00002
KE 220609-1d	20.00±0.01	50.0±0.4	311±3	6.22±0.08	0.00374±0.00005
KE 220609-1e	20.00±0.01	50.0±0.4	125±1	2.49±0.03	0.00221±0.00002
KE 220609-1f	20.00±0.01	50.0±0.4	100±1	2.00±0.03	0.0018152±0.0000009
KE 220610-1	20.00±0.01	50.0±0.4	281±3	5.62±0.08	0.00363±0.00002
KE 220621-2a	20.00±0.01	50.0±0.4	259±3	5.17±0.07	0.00317±0.00002
KE 220621-2b	20.00±0.01	50.0±0.4	401±4	8.02±0.11	0.004642±0.000009
KE 220621-2c	20.00±0.01	50.0±0.4	130±1	2.60±0.04	0.002091±0.000001
KE 220622-1	20.00±0.01	50.0±0.4	223±2	4.47±0.06	0.00346±0.00005
KE 220622-2b	5.00±0.01	50.0±0.4	384±4	7.68±0.10	0.00152±0.00001
KE 220622-2c	5.00±0.01	50.0±0.4	118±1	2.37±0.03	0.000562±0.000001
KE 220623-1	5.00±0.05	50.0±0.4	177±2	3.54±0.05	0.0008265±0.0000009
KE 220624-1a	5.00±0.05	50.0±0.4	234±3	4.68±0.06	0.00144±0.00003
KE 220624-1b	5.00±0.05	50.0±0.4	321±4	6.42±0.09	0.00176±0.00004
KE 220624-1c	5.00±0.05	50.0±0.4	350±4	7.00±0.10	0.00202±0.00005
KE 220627-1a	25.00±0.01	50.0±0.4	312±3	6.25±0.09	0.00533±0.00009
KE 220627-1b	25.00±0.01	50.0±0.4	125±1	2.50±0.03	0.00379±0.00003
KE 220627-1c	25.00±0.01	50.0±0.4	282±3	5.64±0.08	0.00543±0.00002
KE 220627-1d	25.00±0.01	50.0±0.4	188±2	3.76±0.05	0.00439±0.00001
KE 220627-1e	25.00±0.01	50.0±0.4	345±4	6.89±0.09	0.005763±0.000005
KE 220628-1a	16.00±0.01	50.0±0.4	304±3	6.09±0.08	0.0027±0.0001
KE 220628-1c	16.00±0.01	50.0±0.4	275±3	5.49±0.07	0.00263±0.00003
KE 220628-1d	16.00±0.01	50.0±0.4	183±2	3.67±0.05	0.00192±0.00003
KE 220628-1e	16.00±0.01	50.0±0.4	337±4	6.74±0.09	0.002889±0.000001
KE 220629-2c	5.00±0.01	50.0±0.4	200±2	4.01±0.05	0.00095±0.00001

Table S3 (continued). Schedule of experiments: PPN in n-octanol. Experiments were conducted with the Varian GC-ECD.

Internal reference	T (°C)	V_l (mL)	Φ (mL min^{-1})	$\dfrac{\Phi}{V_l}$ (min^{-1})	$\dfrac{\mathrm{d}}{\mathrm{d}t}\ln\left(\dfrac{c_{g,0}}{c_{g,t}}\right)$ (min^{-1})
KE 220711-1b	8.50±0.01	50.0±0.4	118±1	2.37±0.03	0.000843±0.000009
KE 220711-1c	8.50±0.01	50.0±0.4	267±3	5.34±0.07	0.00155±0.00001
KE 220711-1d	8.50±0.01	50.0±0.4	178±2	3.56±0.05	0.0010546±0.0000009
KE 220712-1a	8.50±0.01	50.0±0.4	327±4	6.55±0.09	0.00197±0.00002
KE 220712-1b	8.50±0.01	50.0±0.4	238±3	4.77±0.06	0.00162±0.00002
KE 220712-1c	8.50±0.01	50.0±0.4	358±4	7.16±0.10	0.00223±0.00004
KE 220712-2b	12.50±0.01	50.0±0.4	121±1	2.43±0.03	0.001046±0.000002
KE 220713-1a	12.50±0.01	50.0±0.4	273±3	5.46±0.07	0.00214±0.00002
KE 220713-1b	12.50±0.01	50.0±0.4	182±2	3.64±0.05	0.00168±0.00002
KE 220713-1c	12.50±0.01	50.0±0.4	334±4	6.68±0.09	0.0025±0.0001
KE 220713-1d	12.50±0.01	50.0±0.4	152±2	3.03±0.04	0.00161±0.00008
KE 220713-1e	12.50±0.01	50.0±0.4	243±3	4.86±0.07	0.00206±0.00007
KE 220713-2	5.00±0.01	50.0±0.4	147±2	2.94±0.04	0.000682±0.000001
KE 220714-1a	5.00±0.01	50.0±0.4	252±3	5.05±0.07	0.00127±0.00002
KE 220714-1b	5.00±0.01	50.0±0.4	211±2	4.23±0.06	0.00105±0.00004
KE 220714-1c	5.00±0.01	50.0±0.4	382±4	7.64±0.10	0.00181±0.00003
KE 220714-1d	5.00±0.01	50.0±0.4	265±3	5.29±0.07	0.00129±0.00003
KE 220714-1e	5.00±0.01	50.0±0.4	306±3	6.12±0.08	0.00167±0.00006
KE 220718-1b	5.00±0.01	50.0±0.4	354±4	7.09±0.10	0.00122±0.00003
KE 220718-1c	5.00±0.01	50.0±0.4	331±4	6.62±0.09	0.00142±0.00001
KE 220718-1d	5.00±0.01	50.0±0.4	401±4	8.02±0.11	0.001641±0.000001
KE 220719-1a	5.00±0.01	50.0±0.4	318±3	6.36±0.09	0.00167±0.00002
KE 220719-1b	5.00±0.01	50.0±0.4	365±4	7.30±0.10	0.00195±0.00004
KE 220719-1c	5.00±0.01	50.0±0.4	413±5	8.26±0.11	0.00206±0.00006
KE 220719-2	5.00±0.01	100.0±0.6	94±1	0.94±0.01	0.000285±0.000001
KE 220720-1a	5.00±0.01	100.0±0.6	176±2	1.76±0.02	0.00062±0.00001
KE 220720-1b	5.00±0.01	100.0±0.6	129±1	1.29±0.02	0.000466±0.000007
KE 220720-1c	5.00±0.01	100.0±0.6	188±2	1.88±0.02	0.000667±0.000008

Table S3 (continued). Schedule of experiments: PPN in n-octanol. Experiments were conducted with the Varian GC-ECD.

Internal reference	T (°C)	V_l (mL)	Φ (mL min^{-1})	$\dfrac{\Phi}{V_l}$ (min^{-1})	$\dfrac{\mathrm{d}}{\mathrm{d}t}\ln\left(\dfrac{c_{g,0}}{c_{g,t}}\right)$ (min^{-1})
KE 220720-1d	5.00±0.05	100.0±0.6	153±2	1.53±0.02	0.000444±0.000001
KE 220721-1b	16.00±0.01	50.0±0.4	257±3	5.14±0.07	0.00235±0.00004
KE 220721-1c	16.00±0.01	50.0±0.4	153±2	3.06±0.04	0.001639±0.000007
KE 220721-1d	16.00±0.01	50.0±0.4	221±2	4.42±0.06	0.00219±0.00002
KE 220725-1a	20.00±0.01	100.0±0.4	148±2	1.48±0.02	0.00140±0.00006
KE 220725-1b	20.00±0.01	100.0±0.4	432±5	4.32±0.05	0.00372±0.00009
KE 220725-1c	20.00±0.01	100.0±0.4	99±1	0.99±0.01	0.00149±0.00003
KE 220725-1d	20.00±0.01	100.0±0.4	185±2	1.85±0.02	0.00206±0.00001
KE 220725-1e	20.00±0.01	100.0±0.4	463±5	4.63±0.05	0.00325±0.00003
KE 220725-1f	20.00±0.01	100.0±0.4	111±1	1.11±0.01	0.001492±0.000001
KE 220726-1a	25.00±0.01	100.0±0.4	150±2	1.50±0.02	0.00350±0.00009
KE 220726-1b	25.00±0.01	100.0±0.4	100±1	1.00±0.01	0.00307±0.00007
KE 220726-1c	25.00±0.01	100.0±0.4	451±5	4.51±0.05	0.0050±0.0001
KE 220726-1d	25.00±0.01	100.0±0.4	201±2	2.01±0.02	0.0033±0.0001
KE 220726-1e	25.00±0.01	100.0±0.4	502±6	5.02±0.06	0.00513±0.00006
KE 220726-2	12.50±0.01	100.0±0.4	102±1	1.02±0.01	0.000622±0.000002
KE 220727-1a	12.50±0.01	100.0±0.4	204±2	2.04±0.02	0.00115±0.00001
KE 220727-1b	12.50±0.01	100.0±0.4	450±5	4.50±0.05	0.00190±0.00002
KE 220727-1c	12.50±0.01	100.0±0.4	144±2	1.44±0.02	0.00088±0.00003
KE 220727-1d	12.50±0.01	100.0±0.4	390±4	3.90±0.05	0.00174±0.00007
KE 220727-1e	12.50±0.01	100.0±0.4	240±3	2.40±0.03	0.00131±0.00003
KE 220727-2	8.50±0.01	100.0±0.4	101±1	1.01±0.01	0.000438±0.000001
KE 220728-1a	8.50±0.01	100.0±0.4	296±3	2.96±0.03	0.00118±0.00004

Table S4. Schedule of experiments: PPN in n-octanol containing ~(0.6±0.2) mM of α-tocopherol. Experiments were conducted with the Varian GC-ECD.

Internal reference	T (°C)	V_l (mL)	Φ (mL min^{-1})	$\dfrac{\Phi}{V_l}$ (min^{-1})	$\dfrac{\mathrm{d}}{\mathrm{d}t}\ln\left(\dfrac{c_{\mathrm{g},0}}{c_{\mathrm{g},t}}\right)$ (min^{-1})
KE 220809-1b	20.00±0.01	100.0±0.4	123±1	1.23±0.01	0.0027±0.0002
KE 220809-1c	20.00±0.01	100.0±0.4	278±3	2.78±0.03	0.00345±0.00002
KE 220809-1d	20.00±0.01	100.0±0.4	185±2	1.85±0.02	0.003015±0.000004
KE 220810-1a	20.00±0.01	100.0±0.4	339±4	3.39±0.04	0.0033±0.0001
KE 220810-1b	20.00±0.01	100.0±0.4	197±2	1.97±0.02	0.00310±0.00009
KE 220810-1c	20.00±0.01	100.0±0.4	247±3	2.47±0.03	0.00341±0.00005
KE 220810-1d	20.00±0.01	100.0±0.4	370±4	3.70±0.04	0.00404±0.00003
KE 220810-1e	20.00±0.01	100.0±0.4	123±1	1.23±0.01	0.003100±0.000007
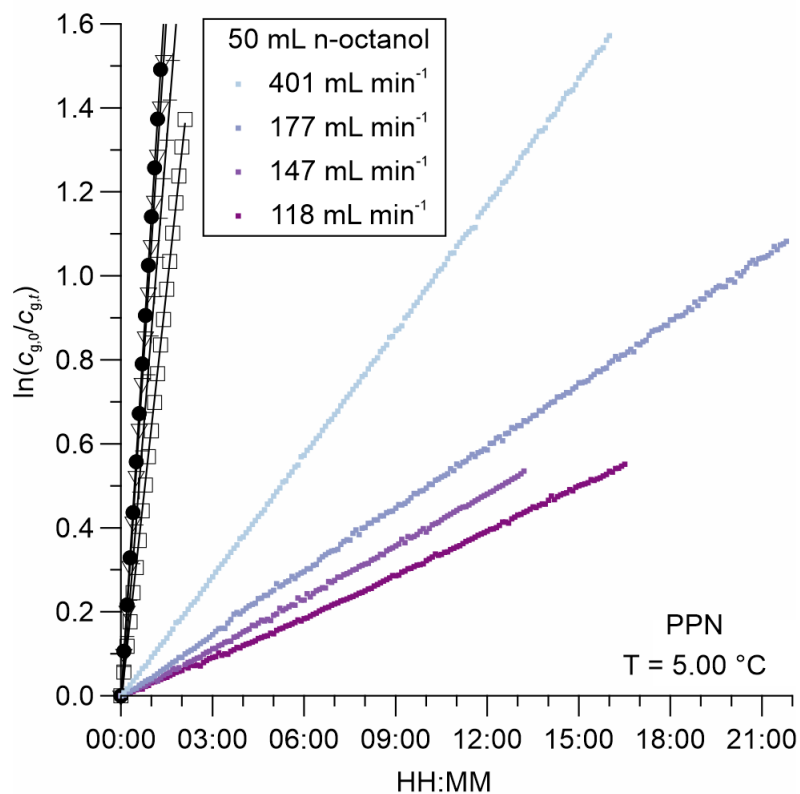
Figure S1. Plots of $\ln(c_{g,0}/c_{g,t})$ versus t for PPN, observed in overnight experiments downstream from 50 mL of n-octanol at 5.00 °C for four different volumetric flow rates. Each data point shown is derived from the peak area of an individual chromatogram, of which there were between 119 and 219 at each flow rate. The data from Figure 3 are superimposed in black colour.
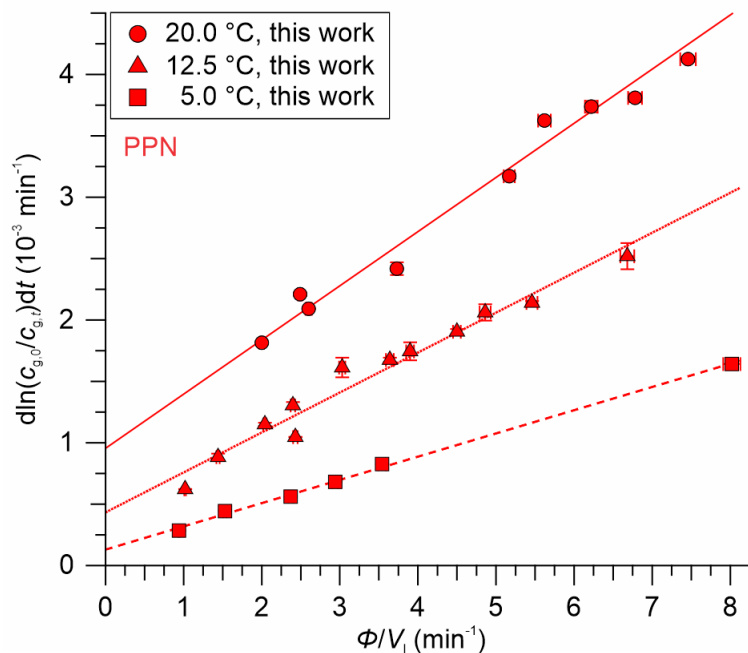
Figure S2. Plots of $d\ln(c_{g,0}/c_{g,t})/dt$ versus Φ/V_l for PPN in n-octanol at 20.00 °C (●), 12.50 °C (▲), and
5.00 °C (■).
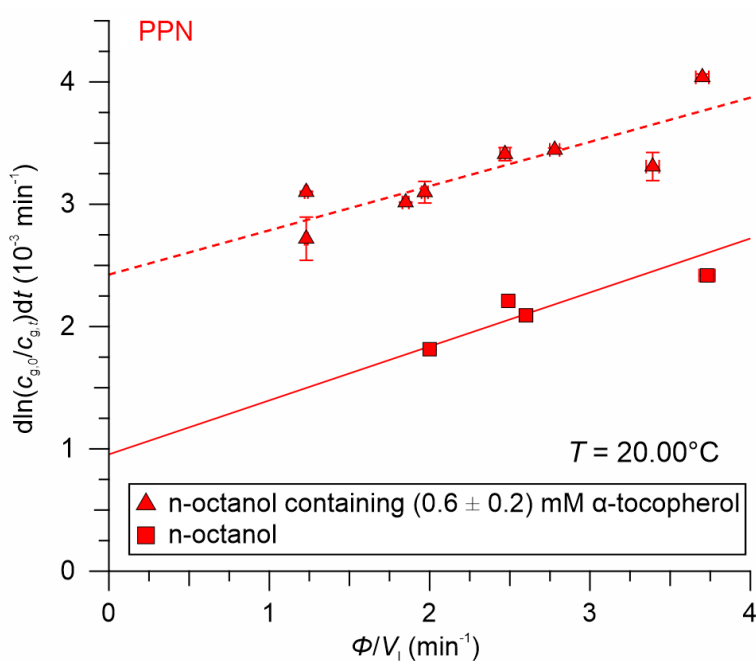
Figure S3. Effect of adding Vitamin E on plots of $d\ln(c_{g,0}/c_{g,t})/dt$ versus Φ/V_l for PPN in n-octanol at
20.00 ºC. Results with unadulterated n-octanol are shown as (■), whereas results with n-octanol containing
~(0.6±0.2) mM of α-tocopherol are shown as (▲).

125 **Table S5.** Dimensionless Henry's law constants of PAN in deionized water, $H_{S,aq}^{CCcc}$(PAN). N/A = not available. n/d = not determined.

	$H_{S,aq}^{CCcc}$(PAN) (unitless)	
Reference	**293.15 K**	**278.15 K**
(Lee, 1984)	98.3±4.8 (295 K)	n/d
(Kames et al., 1991)	97.4±3.6	N/A
(Kames and Schurath, 1995)	97.9±2.0	N/A
This work	101±10	269±13

Table S6. Dimensionless Henry's law constants of PPN in deionized water, $H_{S,aq}^{CCcc}$(PPN). N/A = not
130 available.

	$H_{S,aq}^{CCcc}$(PPN) (unitless)					
Reference	**298.15**	**293.15 K**	**289.15 K**	**285.65 K**	**281.65 K**	**278.15 K**
(Kames and Schurath, 1995)	N/A	70.8±1.5	N/A	N/A	N/A	N/A
This work	36.5±1.1	64.2±4.4	74.5±4.5	96.4±1.7	114.7±7.1	160.1±5.6

Table S7. Dimensionless Henry's law constants of PPN in n-octanol, $H_{S,oct}^{CCcc}$(PPN).

	$H_{S,oct}^{ccCC}$(PPN) (unitless)					
Reference	**298.15 K**	**293.15 K**	**289.15 K**	**285.65 K**	**281.65 K**	**278.15 K**
This work	(2.15±0.11) $\times10^3$	(2.35±0.21) $\times10^3$	(2.98±0.19) $\times10^3$	(3.07±0.18) $\times10^3$	(3.62±0.26) $\times10^3$	(4.65±0.36) $\times10^3$

135 **Table S8.** Loss rate constants of PPN at 293.15 K.

Compound and solvent / medium	k $(10^{-4}\ s^{-1})$
PPN in DI water	3.8±0.6
PPN in n-octanol	0.18±0.03
PPN in n-octanol containing ~(0.6±0.2) mM α-tocopherol	0.40±0.04
PPN in air (Kabir et al., 2014)	1.7

Table S9a. Estimated lifetimes of PAN with respect to wet deposition in the atmosphere at 293 K.

Type	L $(g\ m^{-3})$	$H_S^{CCcc}(PAN) \times L$	$k_{l,aq}(PAN)$ $(10^{-4}\ s^{-1})$	$\tau_{wet}(PAN)$ $=\left(k_{l,aq} \times H_S^{CCcc} \times L\right)^{-1}$
Aerosol (low load)	2.4×10^{-6} (Nenes et al., 2021)	2.4×10^{-10}	3.8 (this work)	350 ky
Aerosol (high load)	1.0×10^{-4} (Nenes et al., 2021)	1.0×10^{-8}	3.8 (this work)	8.3 ky
Stratus clouds (continental)	0.28 (Hess et al., 1998)	2.8×10^{-5}	3.8 (this work)	3.0 y
Stratus clouds (maritime)	0.30 (Hess et al., 1998)	3.0×10^{-5}	44 (Kames and Schurath, 1995)	87 d
Cumulus clouds (continental, clean)	0.26 (Hess et al., 1998)	2.6×10^{-5}	3.8 (this work)	3.2 y
Cumulus clouds (continental, polluted)	0.30 (Hess et al., 1998)	3.0×10^{-5}	3.8 (this work)	2.8 y
Cumulus clouds (maritime)	0.44 (Hess et al., 1998)	4.4×10^{-5}	44 (Kames and Schurath, 1995)	59 d
Cumulonimbus clouds (Java)	3.0 (Rosenfeld and Lensky, 1998)	3.0×10^{-4}	3.8 (this work)	101 d
Fog	0.058 (Hess et al., 1998)	5.8×10^{-6}	3.8 (this work)	14 y
Fog (Po Valley)	0.3 (Wobrock et al., 1992)	3.0×10^{-5}	3.8 (this work)	2.8 y
Fog (maritime)	0.058 (Hess et al., 1998)	5.8×10^{-6}	44 (Kames and Schurath, 1995)	1.2 y
Fog (maritime)	0.8 (Dimitrova et al., 2021)	8.1×10^{-5}	44 (Kames and Schurath, 1995)	33 d
Fog (maritime)	1.8 (Osthoff et al., 2006)	1.8×10^{-4}	44 (Kames and Schurath, 1995)	14 d

Table S9b. Estimated lifetimes of PPN with respect to wet deposition in the atmosphere at 293 K.

Type	L (g m^{-3})	H_S^{CCcc} (PPN) $\times L$	$k_{l,aq}$ (PPN) (10^{-4} s^{-1})	τ_{wet} (PPN) $= \left(k_{l,aq} \times H_S^{CCcc} \times L \right)^{-1}$
Aerosol (low load)	2.4×10^{-6} (Nenes et al., 2021)	1.5×10^{-10}	3.8 (this work)	540 ky
Aerosol (high load)	1.0×10^{-4} (Nenes et al., 2021)	6.4×10^{-9}	3.8 (this work)	13 ky
Stratus clouds (continental)	0.28 (Hess et al., 1998)	1.8×10^{-5}	3.8 (this work)	4.6 y
Stratus clouds (maritime)	0.30 (Hess et al., 1998)	1.9×10^{-5}	44 (Kames and Schurath, 1995)	137 d
Cumulus clouds (continental, clean)	0.26 (Hess et al., 1998)	1.7×10^{-5}	3.8 (this work)	5.0 y
Cumulus clouds (continental, polluted)	0.30 (Hess et al., 1998)	1.9×10^{-5}	3.8 (this work)	4.3 y
Cumulus clouds (maritime)	0.44 (Hess et al., 1998)	2.8×10^{-5}	44 (Kames and Schurath, 1995)	93 d
Cumulonimbus clouds (Java)	3.0 (Rosenfeld and Lensky, 1998)	1.9×10^{-4}	3.8 (this work)	158 d
Fog	0.058 (Hess et al., 1998)	3.7×10^{-6}	3.8 (this work)	22 y
Fog (Po Valley)	0.3 (Wobrock et al., 1992)	1.9×10^{-5}	3.8 (this work)	4.3 y
Fog (maritime)	0.058 (Hess et al., 1998)	3.7×10^{-6}	44 (Kames and Schurath, 1995)	1.9 y
Fog (maritime)	0.8 (Dimitrova et al., 2021)	5.1×10^{-5}	44 (Kames and Schurath, 1995)	51 d
Fog (maritime)	1.8 (Osthoff et al., 2006)	1.2×10^{-4}	44 (Kames and Schurath, 1995)	23 d

140

Table S10a. Estimated lifetimes of PAN with respect to wet deposition in the atmosphere at 278 K.

Type	L (g m^{-3})	H_S^{CCcc}(PAN) $\times L$	$k_{l,aq}$(PAN) (10^{-4} s^{-1})	τ_{wet}(PAN) $= \left(k_{l,aq} \times H_S^{CCcc} \times L \right)^{-1}$
Aerosol (low load)	2.4×10^{-6} (Nenes et al., 2021)	6.4×10^{-10}	1.8 (this work)	274 ky
Aerosol (high load)	1.0×10^{-4} (Nenes et al., 2021)	2.7×10^{-8}	1.8 (this work)	6.5 ky
Stratus clouds (continental)	0.28 (Hess et al., 1998)	7.5×10^{-5}	1.8 (this work)	2.3 y
Stratus clouds (maritime)	0.30 (Hess et al., 1998)	8.1×10^{-5}	44 (Kames and Schurath, 1995)	33 d
Cumulus clouds (continental, clean)	0.26 (Hess et al., 1998)	7.0×10^{-5}	1.8 (this work)	2.5 y
Cumulus clouds (continental, polluted)	0.30 (Hess et al., 1998)	8.1×10^{-5}	1.8 (this work)	2.2 y
Cumulus clouds (maritime)	0.44 (Hess et al., 1998)	1.2×10^{-4}	44 (Kames and Schurath, 1995)	22 d
Cumulonimbus clouds (Java)	3.0 (Rosenfeld and Lensky, 1998)	8.1×10^{-4}	1.8 (this work)	80 d
Fog	0.058 (Hess et al., 1998)	1.6×10^{-5}	1.8 (this work)	11 y
Fog (Po Valley)	0.3 (Wobrock et al., 1992)	8.1×10^{-5}	1.8 (this work)	2.2 y
Fog (maritime)	0.058 (Hess et al., 1998)	1.6×10^{-5}	44 (Kames and Schurath, 1995)	168 d
Fog (maritime)	0.8 (Dimitrova et al., 2021)	2.2×10^{-4}	44 (Kames and Schurath, 1995)	12 d
Fog (maritime)	1.8 (Osthoff et al., 2006)	4.8×10^{-4}	44 (Kames and Schurath, 1995)	5 d

Table S10b. Estimated lifetimes of PPN with respect to wet deposition in the atmosphere at 278 K.

Type	L (g m^{-3})	H_S^{CCcc}(PPN) $\times L$	$k_{l,aq}$(PPN) (10^{-4} s^{-1})	τ_{wet}(PPN) $= \left(k_{l,aq} \times H_S^{CCcc} \times L \right)^{-1}$
Aerosol (low load)	$2.4{\times}10^{-6}$ (Nenes et al., 2021)	$3.8{\times}10^{-10}$	1.0 (this work)	840 ky
Aerosol (high load)	$1.0{\times}10^{-4}$ (Nenes et al., 2021)	$1.6{\times}10^{-8}$	1.0 (this work)	20 ky
Stratus clouds (continental)	0.28 (Hess et al., 1998)	$4.5{\times}10^{-5}$	1.0 (this work)	7.2 y
Stratus clouds (maritime)	0.30 (Hess et al., 1998)	$4.8{\times}10^{-5}$	44 (Kames and Schurath, 1995)	55 d
Cumulus clouds (continental, clean)	0.26 (Hess et al., 1998)	$4.2{\times}10^{-5}$	1.0 (this work)	7.7 y
Cumulus clouds (continental, polluted)	0.30 (Hess et al., 1998)	$4.8{\times}10^{-5}$	1.0 (this work)	6.7 y
Cumulus clouds (maritime)	0.44 (Hess et al., 1998)	$7.0{\times}10^{-5}$	44 (Kames and Schurath, 1995)	37 d
Cumulonimbus clouds (Java)	3.0 (Rosenfeld and Lensky, 1998)	$4.8{\times}10^{-4}$	1.0 (this work)	244 d
Fog	0.058 (Hess et al., 1998)	$9.3{\times}10^{-6}$	1.0 (this work)	35 y
Fog (Po Valley)	0.3 (Wobrock et al., 1992)	$4.8{\times}10^{-5}$	1.0 (this work)	6.7 y
Fog (maritime)	0.058 (Hess et al., 1998)	$9.3{\times}10^{-6}$	44 (Kames and Schurath, 1995)	283 d
Fog (maritime)	0.8 (Dimitrova et al., 2021)	$1.3{\times}10^{-4}$	44 (Kames and Schurath, 1995)	21 d
Fog (maritime)	1.8 (Osthoff et al., 2006)	$2.9{\times}10^{-4}$	44 (Kames and Schurath, 1995)	9 d

145 **Table S11.** Reactive uptake probabilities of PAN and PPN calculated using Eq. (8-9 10). The water viscosities were obtained from Korson et al. (1969) and those for n-octanol were calculated by linear extrapolation of the above-room temperature data by Venkatesan et al. (2020). Molar volume data were obtained using the PhysChem module of the ACD/Labs percepta platform via the Royal Society of Chemistry's Chemspider web site (2022).

Compound and solvent	T (K)	μ (mPa s)	D_l (10^{-9} m^2 s^{-1})	k_1 (10^{-5} s^{-1})	ω (m s^{-1})	H_S^{CCcc}	γ (10^{-5})
PAN and DI water	278.15	1.5192	0.88	18	221	269	0.2
PAN and DI water	293.15	1.0020	1.4	38	226	101	0.1
PPN and DI water	278.15	1.5192	0.86	10	209	160	0.09
PPN and DI water	293.15	1.0020	1.4	38	214	64	0.09
PAN and n-octanol	278.15	12.2	2.3	0.5	221	1920	0.4
PAN and n-octanol	293.15	9.3	3.2	0.3	226	1010	0.2
PPN and n-octanol	278.15	12.2	2.3	0.3	209	4652	0.7
PPN and n-octanol	293.15	9.3	3.2	1.8	214	2351	1.1

150

References

ChemSpider: http://www.chemspider.com/Chemical-Structure.20713.html and
http://www.chemspider.com/Chemical-Structure.15907.html, access: Aug 8, 2022.

Dimitrova, R., Sharma, A., Fernando, H. J. S., Gultepe, I., Danchovski, V., Wagh, S., Bardoel, S. L., and
155   Wang, S.: Simulations of Coastal Fog in the Canadian Atlantic with the Weather Research and
Forecasting Model, Bound.-Layer Meteor., 181, 443-472, 10.1007/s10546-021-00662-w, 2021.

Hess, M., Koepke, P., and Schult, I.: Optical Properties of Aerosols and Clouds: The Software Package
OPAC, Bulletin of the American Meteorological Society, 79, 831-844, 10.1175/1520-
0477(1998)079<0831:Opoaac>2.0.Co;2, 1998.

160   Kabir, M., Jagiella, S., and Zabel, F.: Thermal Stability of n-Acyl Peroxynitrates, Internat. J. Chem. Kin.,
46, 462-469, 10.1002/kin.20862, 2014.

Kames, J., Schweighoefer, S., and Schurath, U.: Henry's law constant and hydrolysis of peroxyacetyl
nitrate (PAN), J. Atmos. Chem., 12, 169-180, 10.1007/BF00115778, 1991.

Kames, J., and Schurath, U.: Henry's law and hydrolysis rate constants for peroxyacyl nitrates (PANs)
165   using a homogeneous gas-phase source, J. Atmos. Chem., 21, 151-164, 10.1007/BF00696578, 1995.

Korson, L., Drost-Hansen, W., and Millero, F. J.: Viscosity of water at various temperatures, The Journal
of Physical Chemistry, 73, 34-39, 10.1021/j100721a006, 1969.

Lee, Y. N.: Kinetics of some aqueous-phase reactions of peroxyacetyl nitrate, Brookhaven National Lab.,
Upton, NY (USA)BNL-34735; CONF-840489-4; ON:DE84011911, 1984.

170   Nenes, A., Pandis, S. N., Kanakidou, M., Russell, A. G., Song, S., Vasilakos, P., and Weber, R. J.:
Aerosol acidity and liquid water content regulate the dry deposition of inorganic reactive nitrogen,
Atmos. Chem. Phys., 21, 6023-6033, 10.5194/acp-21-6023-2021, 2021.

Osthoff, H. D., Sommariva, R., Baynard, T., Pettersson, A., Williams, E. J., Lerner, B. M., Roberts, J. M.,
Stark, H., Goldan, P. D., Kuster, W. C., Bates, T. S., Coffman, D., Ravishankara, A. R., and Brown, S.
175   S.: Observation of daytime N_2O_5 in the marine boundary layer during New England Air Quality Study
- Intercontinental Transport and Chemical Transformation 2004, J. Geophys. Res., 111, D23S14,
10.1029/2006JD007593, 2006.

Rosenfeld, D., and Lensky, I. M.: Satellite-Based Insights into Precipitation Formation Processes in
Continental and Maritime Convective Clouds, Bulletin of the American Meteorological Society, 79,
180   2457-2476, 10.1175/1520-0477(1998)079<2457:Sbiipf>2.0.Co;2, 1998.

Venkatesan, D., Amarnath D, J., Krishna, T. S., Biswas, P., and Dey, R.: Densities, viscosities and excess
parameters of octanol with alkyl(C1 – C4) acetates at varying temperatures, Journal of Molecular
Liquids, 299, 112221, 10.1016/j.molliq.2019.112221, 2020.

Wobrock, W., Schell, D., Maser, R., Kessel, M., Jaeschke, W., Fuzzi, S., Facchini, M. C., Orsi, G.,

185   Marzorati, A., Winkler, P., Arends, B. G., and Bendix, J.: Meteorological characteristics of the Po

Valley fog, Tellus B: Chemical and Physical Meteorology, 44, 469-488, 10.3402/tellusb.v44i5.15562,

1992.